Chapter 1
The BCS–BEC Crossover and the Unitary Fermi Gas

M. Randeria, W. Zwerger and M. Zwierlein

1.1 Introduction

There has been great excitement about the recent experimental and theoretical progress in elucidating the Bardeen-Cooper-Schrieffer (BCS) to Bose Einstein condensation (BEC) crossover in ultracold Fermi gases. Prior to these cold atom experiments, all known, and reasonably well understood, superconductors and superfluids were firmly in one of the two limits. Either they were well described by the celebrated BCS theory of pairing in Fermi systems, or they could be understood in terms of the BEC of bosons, with repulsive interactions. For the first time, the ultracold Fermi gases exhibited behavior that, with the turn of a knob, could be made to span the entire range from BCS to BEC. While such a crossover had been theoretically predicted, its actual realization in the laboratory was a major advance [1, 2], and led to intense investigation of the properties of the very strongly interacting, unitary regime that lies right in the middle of the crossover. We now understand that the unitary Fermi gas has remarkable universal properties, arising from scale invariance, and has connections with fields as diverse as nuclear physics and string theory.

Our goal in this introductory chapter is to convey the excitement of all these new developments, and to give a brief overview of the field which should also serve to

M. Randeria (✉)
Department of Physics, Ohio State University,
Columbus, OH 43210, USA
e-mail: randeria@mps.ohio-state.edu

W. Zwerger
Physik Department, Technische Universität München,
D-85747 Garching, Germany
e-mail: zwerger@ph.tum.de

M. Zwierlein
Department of Physics, MIT-Harvard Center for Ultracold Atoms and
Research Laboratory of Electronics, MIT, Cambridge, MA 02139, USA
e-mail: zwierlei@mit.edu

W. Zwerger (ed.), *The BCS–BEC Crossover and the Unitary Fermi Gas*,
Lecture Notes in Physics 836, DOI: 10.1007/978-3-642-21978-8_1,

put the contributions in the rest of the book in proper context. Our emphasis is on the theoretical developments, that are the focus of the rest of the book, but we also mention some of the key experimental results.

It is appropriate to begin our discussion with the BCS theory of pairing in a Fermi gas which has been one of the major paradigms of many-body physics since its invention more than 50 years ago [3]. Despite the idealized nature of this model, the BCS theory of fermionic superfluidity has proven to be remarkably successful. In addition to providing a *quantitative* theory of conventional superconductors [4], it has also given a successful *qualitative* description of many other more complex systems. For example, it describes well the pairing interactions in atomic nuclei [5] or in neutron stars [6]. Moreover, it can easily be generalized to nonconventional superfluids, for instance to p-wave, spin-triplet pairing that occurs in Helium-3 [7], some heavy Fermion compounds [8] or in the Ruthenates [9]. The basic physics of BCS has even been applied to pairing of quarks in color superconducting phases expected in the QCD phase diagram at high densities [10].

In quite simple terms, the BCS state of N fermions might be thought of as condensation of $N/2$ fermion pairs that can all occupy the same state: a bound pair with zero center-of-mass momentum. This naive picture of superconductivity as a BEC of pairs has to be treated with great caution, however. Indeed, in the weak coupling regime considered by BCS, the attractive interaction between electrons is much smaller than the Fermi energy. Thus the size of a Cooper pair is larger than the average interparticle spacing by a factor that is of order 10^3 in conventional superconductors. Within the volume occupied by a single pair, there are thus about a billion other pairs. It is therefore impossible to picture the Cooper pairs of BCS theory as bosonic particles. Historically, an explanation of superconductivity in terms of BEC of pairs was put forward by Blatt, Butler and Schafroth [11, 12]. Their theory, however, did not apply to superconducting metals known at that time. In particular, it implied a critical temperature on the order of the Fermi temperature instead of the much smaller observed T_c. It is a legitimate question, however, to ask whether there was something fundamentally wrong with this idea and, if not, whether there are systems in nature that actually have an attractive interaction comparable to or even larger than the Fermi energy.

The idea that a continuous crossover exists between the BCS and BEC limits first arose in the 1960s with the work by Keldysh on exciton condensation (see the contribution by Keldysh in [13]), although the long range Coulomb interaction in that problem makes it somewhat different. In a pioneering paper, Eagles [14] studied superconductivity in metals with a very low electron density, where the attraction between electrons was no longer small compared with the Fermi energy. Independently, Leggett attacked the problem of the BCS–BEC crossover in the context of Helium 3 [15]. Although He-3 is very much in the BCS limit, Leggett wanted to understand to what extent its properties, e.g., the total angular momentum of the superfluid, might be similar to a BEC of diatomic molecules.

In these early papers [14, 15], which are discussed in the contribution by Leggett and Zhang to this volume, it was shown that the BCS-wavefunction continues to provide a qualitatively correct variational description of the pairing correlations

for arbitrary strength of the attractive interaction. The $T = 0$ crossover mean field theory differs from the standard BCS analysis in only one way. Unlike standard BCS, where the chemical potential μ is essentially the non-interacting Fermi energy ε_F, in the crossover theory one has to solve for μ self-consistently, together with the gap equation. One finds that μ decreases monotonically with increasing attraction, going from ε_F in the BCS limit to a *negative* value in the BEC limit, that is one-half the pair binding energy. Thus one obtains a smooth crossover from the weak-coupling BCS limit with large, overlapping Cooper pairs all the way to the strong-coupling BEC regime of tightly bound dimers. There is no singularity in the many-body ground state even at the threshold for a bound state in the two-body problem; collective Cooper pairs have already formed well before that in the many-body problem. In fact, Leggett pointed out that the only possible singularity occurs when the chemical potential goes through zero as a result of strong attraction. More precisely, there is a critical coupling strength on the BEC-side of the crossover, beyond which the fermionic quasiparticle excitations above the superfluid ground state have their minimum at zero rather than at finite momentum.[1] This change in the nature of the fermionic excitation spectrum is of relevance for population imbalanced gases, where it determines the location of the so-called splitting point [17]. For the balanced gas, in turn, no thermodynamic singularities show up at this point unless pairing occurs in a non-zero angular momentum channel. In this case, there is a true quantum phase transition along the crossover from weak to strong coupling, separating a phase where part of the Fermi surface has no gap to one with a gap in the fermionic excitation spectrum for all momenta [18–20].

The evolution of the critical temperature T_c across the BCS–BEC crossover was first addressed by Nozieres and Schmitt-Rink [21], who also argued that pairing preempts a possible gas-liquid instability that might be expected for strong attractive interactions. With the discovery of high temperature superconductors in 1986 and the realization that the pairing interaction in these systems is rather strong in the sense that the pair size is only slightly larger than the average interparticle spacing, the crossover from a BCS picture of fermionic superfluids to a BEC of strongly bound pairs became of interest again [22]. The fact that superconductivity in the cuprates appears upon doping a Mott-insulator with antiferromagnetic order [23], indicates, however, that simple models which start from a Fermi gas with strong attractive interactions are unable to describe these systems in any quantitative manner.

The qualitative structure of the phase diagram of the BCS–BEC crossover in a dilute Fermi gas in the standard three dimensional (3D) case is shown in Fig. 1.1 and was obtained well before the era of cold atom experiments [21–24, 26] (the situation in two dimensions is similar, yet there are fundamental differences compared to the 3D situation. This is due to the fact that the superfluid transition in 2D is of the Berezinskii-Kosterlitz-Thouless type and, moreover, that there is no equivalent of the unitarity limit in 2D, since pair binding appears at arbitrary weak

[1] Within meanfield theory, this occurs when the chemical potential reaches zero. More precise calculations, however, show that the critical coupling strength $1/(k_F a) \simeq 0.8$ beyond which fermionic excitations have their minimum at zero momentum appears at $\mu \simeq -0.54\varepsilon_F$ [16].

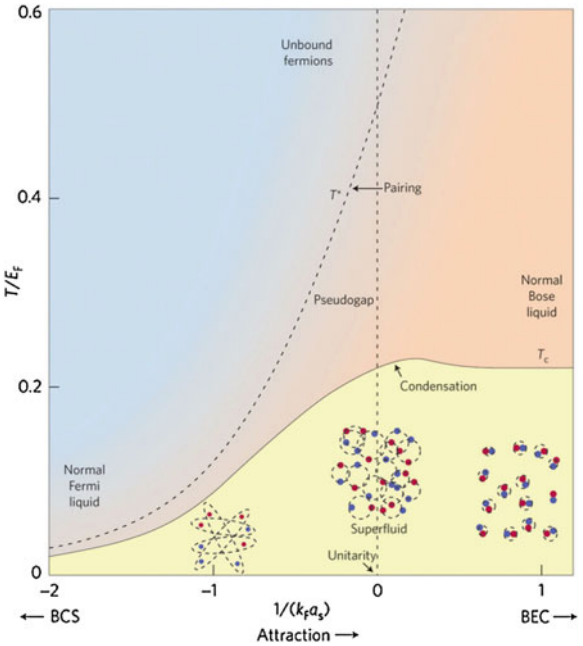

Fig. 1.1 Qualitative phase diagram [24] of the BCS to BEC crossover as a function of the temperature T/T_F and the dimensionless coupling $1/(k_F a)$, where k_F is the Fermi momentum and a the scattering length. The pictures show schematically the evolution of the ground state from the BCS limit with large, spatially overlapping Cooper pairs to the BEC limit with tightly bound molecules. The ground state at unitarity $1/(k_F a) = 0$ has strongly interacting pairs with size comparable to $1/k_F$. As a function of increasing attraction, the pair-formation crossover scale T^* diverges away from the transition temperature T_c below which a condensate exists (Figure from Ref. [25])

attractive interactions [19, 27, 28]). As will become evident from the contributions to these Lecture Notes, many of its features have now been tested experimentally. Moreover, substantial progress has been made within the last few years in understanding the crossover problem on a much deeper level, both in quantitative terms and also conceptually. In dilute Fermi gases, where the range of the potential is much smaller than the interparticle distance k_F^{-1}, the interaction is characterized by a scattering length a. The experimental method for changing a—the Feshbach resonance—is explained in the following Section. At this point, we may simply think of a as being tuned by varying the depth of an attractive square well. For weak attraction one has a negative scattering length and for $1/k_F a \to -\infty$ we are in the BCS limit. The scattering length diverges at the threshold for bound state formation in the two-body problem; this is the unitary point $1/k_F a = 0$. Finally, for strong attraction, $a > 0$ is in fact the size of the two-body bound state in vacuum and in the many-body problem, one is in the BEC limit when $1/k_F a \to +\infty$.

An important point to emphasize here is that although the attraction increases monotonically going from the BCS to BEC regimes (moving from left to right in

Fig. 1.1), both limiting cases are actually weakly interacting. This is clear in the weak attraction BCS limit, but less obvious in the BEC limit, where the strong attraction is resolved by the formation of tightly bound dimers. They have a residual *repulsive* interaction that basically results from the Pauli exclusion of their constituents [24, 27]. The associated scattering length $a_{\rm dd} = 0.6a$ has been determined from an exact solution of the four-body Schrödinger equation [29] and vanishes in the deep BEC limit.[2] The genuinely strongly interacting regime is therefore in the middle of the crossover, near the unitary point $|a| = \infty$. At this point, the superfluid transition temperature $T_c/T_F \simeq 0.22$ is expected to be an appreciable fraction of the Fermi temperature [21, 24]. While more precise calculations based on standard Green function techniques [32, 33], field theoretic expansions around the upper and lower critical dimension [34, 35] or on quantum Monte Carlo methods [36–38] give values $T_c/T_F \simeq 0.16$ that are smaller than these early predictions, the point still remains that such large ratios of the superfluid or superconducting T_c to the bare Fermi energy are unheard of in known condensed matter systems. The unitary gas, which is still basically a fermionic system, in fact has the highest T_c in units of the bare Fermi temperature T_F of all known fermionic superfluids.

A second point that should be stressed is that—as far as the ground state problem is concerned—the BCS–BEC crossover problem is just a simple, smooth evolution from a state with very large pairs to one with small, non-overlapping pairs that behave like point Bosons. By contrast, the normal (i.e., non-superfluid) state crossover is in many ways more subtle. On the BCS-side the formation of pairs and their condensation appears simultaneously. Superfluid order is lost by breaking pairs and—since $T_c \ll T_F$—the corresponding normal state is an ordinary Landau Fermi liquid. By contrast, superfluid order on the BEC side is lost by depleting the condensate but *not* by destroying the bosons. Thus the state above T_c in this limit is a normal Bose gas, where "pairing" still persists. One has to go to a much higher temperature scale T^*, determined by the binding energy, up to logarithmic entropy corrections [22, 24], where the molecular bosons break up into their atomic constituents. The question of how the system above T_c evolves from a normal Fermi liquid to a normal Bose liquid is quite nontrivial and reliable experimental results on this problem have become available only very recently (see the contribution by F. Chevy and C. Salomon in this volume). It was proposed early on that it does so via a pairing pseudogap [39–41] between T_c and T^*. The existence of a pseudogap would be particularly exciting near unitarity where the system can be in a degenerate regime and yet show marked deviations from Fermi-liquid behavior in the temperature range between the phase transition T_c and the the pairing crossover scale T^*. We will say more about this question in Sect. 1.7, where we discuss observable consequences and recent experimental progress. We also discuss there the extent to which these considerations relate to the more complex set of phenomena observed in high T_c superconductivity in the copper-oxide based materials.

[2] A similar result is obtained also in one dimension [30] not, however, in two dimensions, where the repulsive interaction between strongly bound dimers stays finite in the BEC-limit [27, 31].

An independent line of investigation of the problem to understand Fermi gases with strong attractive interactions was started by G. Bertsch in 1999 in the nuclear physics context [42]. As will be discussed in detail in the contribution by Heiselberg, Bertsch suggested to study an attractive Fermi gas with an infinite value of the scattering length as a model to describe low density neutron matter, e.g., in neutron stars. He thus focussed attention on the unitary gas in particular, realizing that–as a result of the zero range nature of the interaction–the Pauli pinciple still guarantees stability despite the infinitely strong attractive interaction and, moreover, that the ground state energy of the unitary gas is necessarily a universal number times the bare Fermi energy [43]. Knowledge of the thermodynamics of the unitary gas realized with ultracold atoms at typical densities $n \simeq 10^{-12}\,\mathrm{cm}^{-3}$ thus has implications for understanding the equation of state of neutron stars at densities that are about twentyfive orders of magnitude larger [44]!

1.2 Feshbach Resonance

Although conceptually important, the BCS–BEC crossover problem was of little direct experimental interest before the era of ultracold atoms, largely because in condensed matter and nuclear physics one has to live with whatever interaction nature provides and there is no way to change it. This situation changed dramatically with the realization that dilute gases of fermionic alkali atoms, such as ^{40}K and ^{6}Li, can be cooled into the degenerate regime [45–50] and that their interatomic interaction can be tuned via a Feshbach resonance [51, 52].

In the following we describe the basic physics of magnetically tunable Feshbach resonances which allow to change the interaction between two different (hyperfine) species of fermions simply by changing a magnetic field. For a more detailed presentation of this subject see, e.g., the recent review by Chin et al. [53]. As we shall see below, in general, one needs a two-channel model to describe a Feshbach resonance: two fermions in the "open channel" coupled to a bound state in the "closed channel". However, essentially all crossover experiments are in the so-called 'broad' Feshbach resonance limit where the width of the resonance is much larger than the Fermi energy. In this limit, an effective single-channel model is sufficient. The two-body interaction is then described by a scattering amplitude of the form $f(k) \simeq -a/(1+ika)$ that only depends on the scattering length a as a single parameter. Typically the scattering length between neutral atoms is of the order of the van der Waals length $r_0 \simeq 50a_0$ and thus much smaller than the typical interparticle spacing $n^{-1/3} \simeq 0.5\,\mu$m in cold gases. Near a Feshbach resonance, however, it is possible that these lengths become comparable.

Quite generally, a Feshbach resonance in a two-particle collision appears whenever a bound state in a closed channel is coupled resonantly with the scattering continuum of an open channel. The ability to tune the scattering length by a change of an external magnetic field B [54] relies on the difference in the magnetic moments of the closed and open channels. Varying B thus changes the position of closed channel bound states relative to the open channel threshold. On a phenomenological

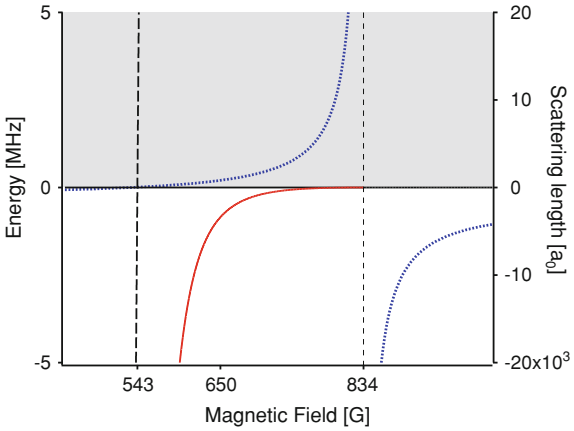

Fig. 1.2 Magnetic field dependence of the scattering length (*blue curve*) between the two lowest magnetic sub-states of ^{6}Li with a Feshbach resonance at $B_0 = 834$ G and a zero crossing at $B_0 + \Delta B = 534$ G. The background scattering length $a_{\rm bg} = -1405\, a_0$ is exceptionally large in this case (where a_0 is the Bohr radius). The energy of the bound state causing the Feshbach resonance is shown in *red*

level, Feshbach resonances are described by an effective pseudopotential between atoms in the open channel with scattering length

$$a(B) = a_{\rm bg}\left(1 - \frac{\Delta B}{B - B_0}\right). \tag{1.1}$$

Here $a_{\rm bg}$ is the off-resonant background scattering length in the absence of the coupling to the closed channel while ΔB and B_0 describe the width and position of the resonance expressed in magnetic field units (see Fig. 1.2).

Taking the specific example of fermionic ^{6}Li atoms, which have electronic spin $S = 1/2$ and nuclear spin $I = 1$, for typical magnetic fields above 500 G, the electron spin is essentially fully polarized by the magnetic field, and aligned in the same direction for the three lowest hyperfine states. Thus, two lithium atoms collide with their electron spins aligned, hence in the triplet configuration. The "incoming" state or open channel is thus part of the triplet interatomic potential. The closed channel consists of states in the singlet potential. Due to the hyperfine interaction, that can trade electron spin for nuclear spin, the two atoms can resonantly tunnel from the triplet into bound states of the singlet potential. This coupling is described by an off-diagonal potential *W(r)*, whose range is on the order of the atomic scale.

As a result of the finite difference $\Delta\mu$ of the magnetic moments in the open and closed channels, a change in the magnetic field by δB amounts to shifting the closed channel energy by $\Delta\mu\delta B$ with respect to the open channel (see Fig. 1.3). Provided that the magnetic field is close to a resonant value B_0 at which a bound state $\phi_{\rm res}(r)$ of the closed channel potential has an energy $E_{\rm res}(B) = \Delta\mu(B - B_0)$ close to zero, this state is resonantly coupled to the open channel scattering state at

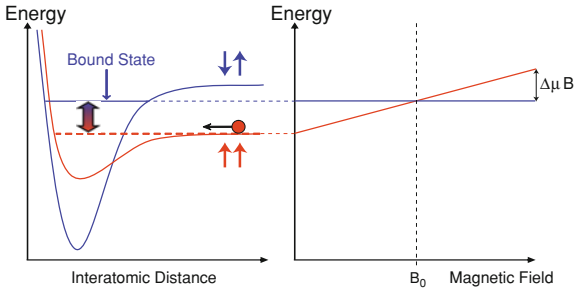

Fig. 1.3 Atoms prepared in the open channel, corresponding to the interaction potential (*in red*), undergo a collision at low incident energy. In the course of the collision the open channel is coupled to the closed channel (*in blue*). When a bound state of the closed channel has an energy close to zero, a scattering resonance occurs. The position of the closed channel can be tuned with respect to the open one, e.g., by varying the magnetic field B

low energies. This coupling leads to a resonant contribution

$$\tan \delta_{\rm res}(k) = \frac{\hbar^2 k}{m r^\star \nu} \tag{1.2}$$

to the scattering phase shift at small momenta $k \to 0$ which is inversely proportional to the detuning $\nu = \Delta\mu(B - B_0)$ away from resonance [55]. The associated characteristic length $r^\star > 0$ is determined by the overlap between the open channel scattering state $|\phi_0\rangle$ and the closed channel bound state $|\phi_{\rm res}\rangle$. More precisely, it is connected to the off-diagonal coupling potential $W(r)$ via [56]

$$\langle \phi_{\rm res}|W|\phi_0\rangle = \frac{\hbar^2}{m}\sqrt{\frac{4\pi}{r^\star}}. \tag{1.3}$$

Its inverse $1/r^\star$ is therefore a measure of how strongly the open and closed channels are coupled. Including the phase shift $\tan \delta_{\rm bg}(k) = -k a_{\rm bg}$ due to scattering in the open channel potential, the total scattering length $a = -\lim_{k\to 0} \tan(\delta_{\rm bg} + \delta_{res})/k$ is of the form

$$a = a_{\rm bg} - \frac{\hbar^2}{m r^\star \nu} \tag{1.4}$$

as given in Eq. 1.1. In particular, the phenomenological width parameter ΔB is determined by the combination $\Delta\mu\Delta B = \hbar^2/(m r^\star a_{\rm bg})$ of the two characteristic lengths $a_{\rm bg}$ and $r^\star$.

In addition to the tunability of the scattering length, Feshbach resonances also allow to form weakly bound dimers by an adiabatic change in the magnetic field that starts from the side with $a < 0$ and slowly crosses the resonance into the regime $a > 0$, where the pseudopotential exhibits a bound state at energy $\varepsilon_b = \hbar^2/(m a^2)$ [53]. The corresponding bound state has a finite closed channel

admixture $\sqrt{Z}\ \phi_{\rm res}$. Close to the resonance, where the scattering length is dominated by the resonant contribution in Eq. 1.4, the binding energy

$$\varepsilon_b = \frac{\hbar^2}{ma^2} = \big(\Delta\mu(B - B_0)\big)^2/\varepsilon^\star + \ldots \tag{1.5}$$

of the weakly bound state vanishes quadratically, with characteristic energy $\varepsilon^\star = \hbar^2/m(r^\star)^2$. The associated closed channel admixture Z is thus given by

$$Z = -\frac{\partial\varepsilon_b}{\partial v} \simeq = 2\frac{|v|}{\varepsilon^*} = 2\frac{r^*}{|a_{\rm bg}|}\ \frac{|B - B_0|}{|\Delta B|}, \tag{1.6}$$

remaining much smaller than one over the magnetic field range $|B - B_0| \lesssim |\Delta B|$ for the typical Feshbach resonances that obey $r^\star \ll |a_{\rm bg}|$ [55].

The discussion so far is based on two-body scattering only. In order to define the notion of a broad Feshbach resonance, however, we have to take into account that at a finite density of the fermionic atoms, the typical relative momenta are of order k_F. Now, the two-particle scattering amplitude

$$f(k) = \frac{1}{k\cot\delta_0(k) - ik} \to \frac{-1}{1/a + r^\star k^2 + ik}. \tag{1.7}$$

near a Feshbach resonance has the parameter $r^\star$ introduced in Eq. 1.2 as an effective range parameter [56]. The condition that the scattering amplitude $f(k_F)$ near the Fermi energy is only determined by the scattering length a and the universal contribution ik that limits the scattering cross section to its maximum value $4\pi/k^2$ at $a = \infty$, therefore requires $k_F r^\star \ll 1$. This is the condition for a 'broad' Feshbach resonance, which only involves the many-body parameter $k_F r^\star$ [56]. In quantitative terms, the Fermi wavelength $\lambda_F = 2\pi/k_F$ of dilute gases is of order μm, while $r^\star$ is typically on the order of or even smaller than the effective range r_e of the interaction. The condition $k_F r^\star \ll 1$ is therefore very well obeyed and characterizes the *low density* limit that is relevant in ultracold gases. A very important point to realize in this context is that the broad Feshbach resonance limit is precisely opposite to that encountered in conventional superconductors. In the latter case, the role of the characteristic energy $\varepsilon^\star$ beyond which the attractive interaction is cutoff is played by the Debye energy $\hbar\omega_D$. Since the ratio $\hbar\omega_D/\varepsilon_F$ is typically very small, pairing in conventional superconductors is described by a model with $k_F r^\star \gg 1$, i.e. one is in the *high-* rather than in the low-density limit. There is again a kind of universality in this limit provided one is the weak coupling regime where the resulting pairs are much larger than the interparticle distance. This is connected with the fact that in weak coupling only properties right *at* the Fermi surface are relevant. Then, a reduced BCS model is applicable for which mean field theory becomes exact and dimensionless ratios like the $2\Delta/k_B T_c = 3.52$ are universal.

Experimentally, a crucial requirement for reaching the regime $k_F|a| \gg 1$ in practice is the stablity of fermionic gases near a Feshbach resonance. If two-body losses are negligible, the lifetime of ultracold gases is limited by three-body losses, where

two of the colliding atoms fall into a deeply bound state. To ensure energy-momentum conservation, a third atom has to be present in order to take away the large excess binding energy. For bosons, the three-body loss rate $K_3 \sim (na^2)^2$ increases strongly with density and scattering length, thus preventing one from reaching the strongly interacting regime $n^{1/3}a \gg 1$ with Feshbach resonances. Fortunately, for fermions the situation is reversed. In fact, their lifetime is particularly *large* near Feshbach resonances because the Pauli principle forbids two fermions of the same kind to be at the same place [29]. Typical lifetimes can in fact reach over half a minute for ^{6}Li [57].

1.3 Universality and Scale Invariance

As described above, the BCS–BEC crossover in dilute Fermi gases can be tuned by changing the scattering length a. Since the interaction in the broad Feshbach resonance limit has a as the single parameter, purely dimensional arguments imply that all measurable quantities can be written in a "universal" form; for instance the free energy per particle must be the form $F(T, V, N)/N = \varepsilon_F \mathscr{F}(T/T_F, 1/k_F a)$. Here $\mathscr{F}(\theta, x)$ is a dimensionless function of the scaled temperature $\theta = T/T_F$ and the dimensionless coupling $x = 1/k_F a$, where $k_B T_F = \varepsilon_F = \hbar^2 k_F^2/2\mathrm{m}$ is the non-interacting Fermi energy (or temperature), and $k_F = (3\pi^2 n)^{1/3}$ is the Fermi momentum corresponding to a density n. In concrete terms, universality in this context implies that functions like $\mathscr{F}(\theta, x)$ are independent of any microscopic details up to corrections of order $(k_F r^*)^2$. Thus, for example, the equation of state of ^{40}K and ^{6}Li, which are both in the broad Feshbach resonance limit $k_F r^\star \ll 1$, should be identical across the entire crossover if expressed in scaled variables θ and x.

More generally, the notion of universality is usually associated with physics near a continuous phase transition, where a diverging length scale gives rise to a behavior that is insensitive to microscopic details. Phrased in these terms, the origin of universality of strongly interacting fermions near a Feshbach resonance was elucidated by Nikolic and Sachdev [58]. As explained in detail in the contribution by Sachdev to this volume, universality is tied to the existence of a quantum critical point at unitarity when the chemical potential vanishes, i.e. the gas is at zero density. Associated with the three relevant perturbations around this fixed point, the complete thermodynamics and phase diagram is then a universal function of temperature T, the deviation from unitarity, the chemical potential μ and the external field h that is conjugate to an imbalance in the density of the two spin components [58].

As pointed out by Bertsch, a subject of particular interest in itself is the unitary gas at infinite scattering length. At the two-body level, this is the critical coupling for the appearance of a bound state. In the many-body problem, this point seems not to have any special significance at first sight, since all the thermodynamic properties are continuous across the particular value $1/k_F a = 0$ of the dimensionless coupling constant. A closer look however, reveals that there are additional symmetries precisely at infinite scattering length. In fact, if the interaction near a Feshbach resonance is modelled by a two-channel description in which two atoms are transformed

into a closed channel 'molecule' and vice versa, the bosonic field associated with the closed channel is massless at zero detuning $\nu = 0$. As a result, the unitary gas is a non-relativistic field theory which is scale-invariant at $k_F a = \infty$, as realized by Son and Nishida and by Werner and Castin [59–61]. The origin and consequences of scale invariance, in particular in the presence of a harmonic trapping potential, are discussed in detail in the contribution by Castin and Werner. In a homogeneous situation, scale invariance implies that the kinetic and interaction energy terms in the Hamiltonian have identical scaling dimension. A rescaling $\mathbf{x} \to \lambda \mathbf{x}$ of the coordinates by an arbitrary factor λ thus results in a simple change of the Hamiltonian by $H \to H/\lambda^2$, as if the two-body interactions were of a pure power law form $\sim 1/r^2$. Note, however, that in systems with pure $1/r^2$-interactions scale invariance holds for any value of the interaction strength and for *any* dimension. For contact interactions $\sim g\delta(\mathbf{x})$ in turn, scale invariance in three and also in one dimension requires either zero or infinite coupling $g = \infty$, while in *two* dimensions it again holds for arbitrary coupling strength, as pointed out earlier by Pitaevskii and Rosch [62]. Within a space-time formulation, scale-invariant, non-relativistic many-body problems are invariant under the transformation $\mathbf{x} \to \lambda \mathbf{x}$ and $t \to \lambda^2 t$. More precisely, the full symmetry group of the unitary gas is known as the Schrödinger group which is the analogue, for Galilean invariant systems, of the conformal group.

Being a continuous symmetry, scale invariance leads to a conservation law by Noether's theorem. The associated conservation of the 'dilaton current' implies that the trace of the energy-momentum tensor vanishes. As a result, the pressure $p = 2\varepsilon/3$ of the non-relativistic, unitary Fermi gas is simply proportional to its energy density ε, a relation which has first been derived using thermodynamic arguments by Ho [63]. Note that the relation holds at arbitrary temperature and is identical to that which is usually associated with an ideal (quantum or classical) gas, even though the system is very strongly interacting. Apart from the simple relation between pressure and energy density, the combination of scale and conformal invariance also has the surprising consequence that the bulk viscosity ζ of the unitary gas vanishes identically [64, 65]. As a result, a unitary gas in an isotropic trap will expand without any generation of entropy after the trap potential is removed. This is discussed in detail in the contributions by Castin and Werner and by Nishida and Son.

1.4 Thermodynamics and Critical Temperature

Following the first experimental realizations of degenerate Fermi gases in the strongly interacting regime near a Feshbach resonance [1, 2, 66–69], quite a lot of effort has been spent to measure the thermodynamic properties and to precisely determine the universal numbers that characterize the unitary gas in particular. From the theory point of view, this is the most interesting and also challenging problem due to the absence of a small expansion parameter. The ground state of a balanced gas with equal densities of the two spin components is a superfluid which is adiabatically connected to the BCS-type superfluid in the weak coupling limit $k_F a \to 0^-$. On purely dimensional grounds, the ground state energy density $\varepsilon = \xi_s \varepsilon^{(0)}$ is a pure number $\xi_s < 1$—called

the Bertsch parameter—times the energy density $\varepsilon^{(0)} = 3n\varepsilon_F/5$ of the non-interacting Fermi gas with the same density n (the subscript in ξ_s is a reminder of the fact that the parameter refers to the superfluid state). Due to the relation $p = 2\varepsilon/3$ and the Gibbs-Duhem relation $N\mu = F + pV$, the universal number ξ_s also determines the factor by which the ground state pressure or the chemical potential of the unitary gas is reduced compared to its value in an ideal, non-interacting Fermi gas. Moreover, the zero temperature compressiblity $\boldsymbol{\kappa} = \partial n/\partial\mu$ is enhanced by a factor $1/\xi_s$. As a result, the ratio $c_s = v_F\sqrt{\xi_s/3}$ between the speed of sound and the Fermi velocity is again fixed by the single parameter ξ_s. Superfluid properties, in turn, are associated with new and independent universal ratios. Of particular interest are the critical temperature for the superfluid transition T_c/T_F and the zero temperature gap Δ/ε_F for fermionic quasiparticles.

There are a number of ways to determine the Bertsch parameter ξ_s experimentally, for instance from a measurement of the release energy after expansion of the gas in a trap [70] or—most directly—from in-situ absorption imaging of the density distribution [66]. Indeed, the density profile at unitarity is that of a free Fermi gas with a rescaled size. Due to the inhomogeneous density, the chemical potential μ_{trap} in the trapped gas is decreased by $\sqrt{\xi_s}$ and not by ξ_s as in the homogeneous case. Since the radius $R \sim \sqrt{\mu_{\text{trap}}}$ of the atomic cloud scales with the square root of the chemical potential, attractive interactions at unitarity give rise to a reduction of the cloud radius by a factor $\xi_s^{1/4}$. The values of ξ_s obtained from this and other measurements [71–73] have a considerable uncertainty $\xi_s = 0.4 \pm 0.1$, however, in part due to the difficulty in extrapolating to zero temperature. An extensive analysis of the thermodynamics of both the balanced and the imbalanced gas near unitarity has recently been performed by the group at ENS [74, 75]. As discussed in the contribution by Chevy and Salomon, these measurements indicate a value $\xi_s = 0.41(1)$ for the Bertsch parameter which is close to that obtained from a variety of analytical approximations [43, 76]. They include diagrammatic techniques like the pair fluctuation approach discussed in detail in the contribution by Strinati [77, 78] or Gaussian functional integrals [79, 80]. Very similar values for ξ_s are obtained from both $T = 0$ fixed-node Monte Carlo calculations [81–83] and also from finite temperature Monte Carlo calculations [84]. The latter method is discussed in detail in the contribution by Bulgac, Forbes and Magierski to this volume. The accuracy of this value is challenged, however, both by recent precision experiments of the equation of state at MIT which give $\xi_s = 0.37 \pm 0.01$ and also by quantum Monte Carlo calculations which indicate an upper bound $\xi_s < 0.38$ [85].

A remarkable consequence of the symmetries of the unitary gas that were mentioned above is that, beyond the derivation of some exact relations, they also provide an unexpected route to calculate its thermodynamic properties from a systematic expansion around an upper and a lower critical dimension. This idea is due to Nishida and Son [34] and is explained in detail in their contribution to this volume. It is based on the observation [86] that the unitary gas in four dimensions is an ideal Bose gas while in two dimensions, it is an ideal Fermi gas. Both, in $d = 4$ and in $d = 2$, the unitary Fermi gas is therefore an exactly soluble problem. This surprising

statement can be understood in physical terms by noting that in four dimensions a two-particle bound state in a zero range potential only appears at infinitely strong attraction. Thus, already at an arbitrary small value of the binding energy, the associated dimer size vanishes, in strong contrast to the situation in $d = 3$, where the size of the two-particle bound state is infinite at unitarity. The unitary Fermi gas in four dimensions is thus a non-interacting BEC, similar to the limit $a \to 0^+$ in three dimensions. The $d = 4 - \varepsilon$ expansion may be complemented by an expansion around the lower critical dimension, which is two for the present problem [35, 86, 87]. Indeed, for $d \leq 2$ a bound state at zero binding energy appears for an arbitrary weak attractive interaction and an expansion around $d = 2 + \varepsilon$ is thus effectively one around the non-interacting Fermi gas. For quantitatively reliable results in the relevant case $d = 3$, the $\varepsilon = 4 - d$ expansion has been extended up to three loops [88]. Within a Pade resummation that takes into account the known behavior in the limit $d \to 2^+$, the resulting value is $\xi_s = 0.36 \pm 0.02$ [89] which agrees very well with the most precise experimental number available at this point. The result $\xi_s = 0.36$ has in fact been obtained within a diagrammatic calculation based on the Luttinger-Ward approach [33]. The conserving nature of the approximation guarantees that all thermodynamic relations are obeyed. Moreover, the approximation respects the exact Tan relations that hold for Fermions with contact interactions, as discussed in the following section. The Luttinger-Ward formulation thus provides an internally consistent and quantitatively reliable picture of the thermodynamics along the full BCS–BEC crossover, both in the normal and in the superfluid phase and at arbitrary values of the coupling $1/k_F a$.

With increasing temperature, superfluidity will eventually be lost. In the balanced gas, the transition to the normal state is continuous along the full BCS–BEC crossover and the associated critical exponents are those of the 3D XY-model. At unitarity, the ratio T_c/T_F between the critical temperature and the bare Fermi temperature is again a universal number. Early calculations, based on including Gaussian fluctuations beyond mean field theory, gave values $T_c/T_F \simeq 0.22$ [21, 24]. They are close to the result $T_c/T_F = 0.218$ reached in the BEC-limit, where strongly bound dimers undergo an ideal Bose-Einstein condensation. More precise results, which take into account the interaction between non-condensed pairs, have been obtained by Haussmann within the Luttinger-Ward approach [32, 33]. Depending on whether the superfluid transition is approched from above or below, the critical temperature of the unitary gas is found to be $T_c/T_F = 0.15$ or 0.16, The apparent first order nature of the transition is clearly an artefact of self-consistent Green function methods but, fortunately, the range of temperatures where the normal state still appears stable in the presence of a finite superfluid order parameter is rather small except on the BEC-side near $k_F a \simeq 1$ [33]. In fact, it is an unsolved challenge to develop conserving approximations that properly account for both the gapless nature of excitations in the symmetry broken phase and the continuous nature of the superfluid transition, a problem that appears already in the classic theory of weakly interacting Bose gases [33, 90]. The value $T_c/T_F \simeq 0.16$ is close to that obtained by quantum Monte Carlo methods, which give $T_c/T_F = 0.152(7)$ [36, 37] or $T_c/T_F = 0.171(5)$ in more recent calculations [38]. Note that in a trap, due to the

increased density at the center, the ratio between T_c and the Fermi temperature of the trap $\widetilde{T}_F$ is higher, close to $T_c/\widetilde{T}_F \simeq 0.21$ [91]. Similarly, since the local value of T_F decreases upon approaching the trap edge, the gas becomes less degenerate there. The critical entropy $S(T_c) \simeq 1.6Nk_B$ necessary for reaching the superfluid transition is therefore considerably larger than the universal value $S(T_c) \simeq 0.7Nk_B$ of the homogeneous gas [33]. As a final example of the universal numbers which characterize the unitary gas, we mention the zero temperature excitation gap Δ for fermionic excitations. The theoretically predicted value $\Delta \simeq 0.46\varepsilon_F$ from both the Luttinger-Ward approach [33] and Monte Carlo calculations [92] agrees rather well with the experimental result $\Delta \simeq 0.44\varepsilon_F$ obtained by RF-spectroscopy [93], as discussed further in Sect. 1.7.

We conclude this Section with qualitative insights on why and how the quantitative results on crossover thermodynamics discussed above differ from those obtained from the simplest BCS-Leggett mean field theory (MFT). In the BCS limit $1/k_Fa \to -\infty$ there are two features that MFT fails to capture. First, the numerical pre-factor in the gap $\Delta \simeq \varepsilon_F \exp(-\pi/2k_F|a|)$ is overestimated. The polarization of the medium, described diagramatically by particle-hole (p-h) fluctuations, effectively weakens the attractive interaction [94, 95]. This reduces both the gap and the critical temperature by a factor $(4e)^{1/3} \simeq 2.2$, leaving the ratio $2\Delta/T_c$ unchanged. (Remarkably, it seems that p-h fluctuations may not have a significant effect on T_c [96] at unitarity.) Secondly, the weak-coupling MFT ground state energy omits corrections perturbative in $k_F|a|$ but includes the exponentially small, non-perturbative pairing contribution. The perturbative "Fermi liquid" corrections are correctly described by Gaussian fluctuations [79] about mean field theory. They have the same form as the classic Lee-Yang-Huang and Galitskii results for the repulsive Fermi gas, but now with a negative scattering length.

In the opposite BEC limit $1/k_Fa \gg 1$, MFT does lead to dimers with a binding energy $\hbar^2/ma^2$. However, the dimer-dimer scattering length is found to be [24, 26] $a_{\rm dd}^{\rm MFT} = 2a$ as compared to the exact result $a_{\rm dd} = 0.6a$ obtained by the solution of the four-fermion problem [29]. This directly impacts the compressibility and the speed of sound in the BEC limit. Gaussian fluctuation theories [79, 80, 97], that work across the entire crossover, are able to approximately account for this renormalization in the BEC limit.

At unitarity, MFT gives a value of $\xi_s^{\rm MFT} = 0.59$ [26] that is much larger than the best estimates ξ_s. This reduction in ground state energy [79] can be attributed to zero point motion of the collective mode and virtual scattering of gapped quasiparticle excitations missing in MFT. Simlarly, at unitarity, the MFT plus Gaussian fluctuation $T_c \simeq 0.2T_F$ [24] neglects critical fluctuations, and thus exceeds the best numerical estimates of T_c.

1.5 Universal Tan Relations

The effort to understand strongly interacting Fermi gases near infinite scattering length has led to a remarkable development in many-body physics that started in a

series of papers by S. Tan in 2005 [98]. He found a number of relations that apply quite generally to two-component fermions with an interaction that has zero range. In particular, Tan has shown that the momentum distribution of each spin-component falls off like C/k^4 at large momenta. The associated constant C, which is called the 'contact', has a simple physical meaning: it is a measure for the probability that two fermions with opposite spin are close together. The contact determines the change of the energy with respect to the interaction strength by a Hellmann-Feynman like relation, the Tan adiabatic theorem. It also allows to calculate the energy from the momentum distribution [99]. A crucial feature of the Tan relations is the fact that they apply to *any* state of the system, e.g., both to a Fermi-liquid or a superfluid state, at zero or at finite temperature and also in a few-body situation. The only change is the value of the contact C. The origin of this universality was elucidated by Braaten and Platter [100]. As described in detail in the contribution by Braaten to this volume, the Tan relations are a consequence of operator identities that follow from a Wilson-Kadanoff operator product expansion of the one-particle density matrix.

The Tan relations have been tested in a number of experiments recently. In a rather direct manner, they may be verified by observing the tail of the momentum distribution obtained in a time-of-flight measurement [101]. Moreover, the fact that a change in the magnetic field results in a linear shift of the closed channel eigenenergy implies, via the Tan adiabatic theorem, that the contact C is proportional to the number of closed channel molecules [102, 103]. As discussed in the contribution by Castin and Werner, this allows to infer the value of the contact along the BCS–BEC crossover from earlier measurements of the closed channel fraction at Rice [104]. A different way of getting access to the contact is via rf-spectroscopy, a method discussed in more detail in Sect. 1.7 In particular, it turns out, that the average shift of the transition frequency compared with those in a free atom due to the effects of interaction, is directly proportional to C [105, 106]. The so-called 'clock-shift' thus basically measures the probability for two atoms to be close together. This probability is not very sensitive as to whether one considers a superfluid or a normal state. In fact, for the unitary gas, the contact C is almost unchanged between the balanced superfluid phase and a normal phase at strong imbalance [106]. This observation provides an understanding of the observation that the average clock-shift hardly changes with imbalance [107]. The contact also shows up as the coefficient of $\omega^{-3/2}$ power-law tail in the rf-spectrum at high frequencies [16, 108, 109], as discussed in the contribution by Braaten. In the presence of non-vanishing final state interactions, the proportionality to the contact still holds. The power law, however, is changed to $\omega^{-5/2}$, which leads to a finite value of the average clockshift obtained from the first moment of the rf spectrum [105, 106]. The consistency of the value for C obtained from either the asymptotics of the momentum distribution or the high frequency part of the rf-spectrum has been verified nicely in experiments performed at JILA [101].

An analog of the Tan relations also hold for Fermi gases in one dimension [110]. Similar to the 3D case, there is again a special value of the coupling where the system is scale invariant, implying an equation of state with $p = 2\varepsilon$. Apart from the trivial non-interacting gas, this appears at both infinite repulsion or attraction. In either one of these limits, the thermodynamics is like that of a single component

Fermi gas: in the repulsive case, the effective Fermi wave vector is doubled because the many-body wave function has to vanish at coincident coordinates not only for Fermions with equal but also for those with opposite spin. In the attractive case, the resulting bound pairs are like hard core bosons due to the underlying Pauli exclusion of their constituents. As discussed in detail in the contribution by Feiguin et al. on the BCS–BEC crossover in one dimension, this is a Tonks-Girardeau gas of dimers.

An extension of the Tan relations has recently also been derived for Bosons with zero range interactions [111]. In addition to the contact, which is a two-body observable, the extended form of the Tan relations for Bosons also involves a three-body parameter that is associated with a—sub-dominant—$1/k^5$-tail of the momentum distribution.

1.6 The Unitary Fermi Gas as a Perfect Fluid?

A quite surprising connection between the physics of ultracold atoms and recent developments in field theory has opened up with the realization that not only equilibrium but also transport properties of the unitary Fermi gas should exhibit universal features. These connections are motivated by the fact that the unitary gas is a non-relativistic field theory which is both scale and conformally invariant [59, 60]. In the relativistic domain, such field theories exhibit quite unique features in their dynamical properties. For example, it has been shown by Policastro, Son and Starinets [112] that the shear viscosity η and the entropy per volume s in a $\mathcal{N} = 4$ supersymmetric Yang-Mills theory in the limit of infinite't Hooft coupling $\lambda = g^2 N \to \infty$ are simply proportional to each other. Their ratio $\eta/s = \hbar/(4\pi k_B)$ is a universal constant independent of temperature. The supersymmetric version of Yang-Mills theory is related by a duality transformation to a theory that involves gravity in a five dimensional space with constant negative curvature called Anti-de Sitter space (AdS-CFT correspondence). Perturbations away from this exactly soluble model typically give rise to larger values of η/s. This observation has prompted Kovtun, Son and Starinets (KSS) to conjecture that the constant $\hbar/(4\pi k_B)$ is a lower bound on the shear viscosity to entropy ratio for a large class of strongly interacting quantum field theories [113] and has motivated the search for the 'perfect fluid' which realizes, or at least comes close to, this bound [114]. A nontrivial example in this context is the standard *SU(3)* Yang-Mills theory for which the associated η/s ratio turns out to be rather close to the KSS bound [115]. Adding fermions to the pure gauge theory, the ratio η/s becomes an experimentally accessible quantity in high-energy, non-central collisions of heavy nuclei. The experimental estimate for the ratio η/s of the quark-gluon plasma is around $0.4\hbar/k_B$, i.e., a factor five above the KSS bound [114]. In fact, the quark-gluon plasma appears to be the most perfect *real* fluid known so far. Surprisingly, ultracold atoms near a Feshbach resonance, at temperatures almost twenty orders of magnitude below that of the quark-gluon plasma, seem to be equally perfect. Questions that were first raised in a string-theory context have thus become of relevance for ultracold atoms. In particular, the unitary Fermi gas provides a

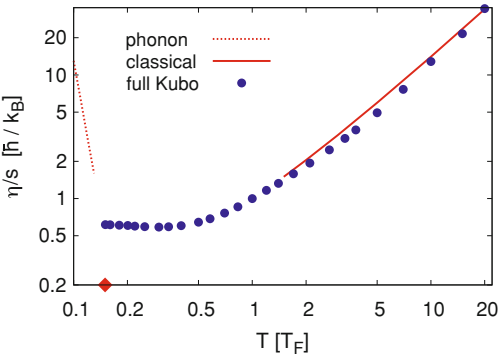

Fig. 1.4 Shear viscosity to entropy ratio η/s (*blue circles*) in comparison with known asymptotes. The *dashed red line* on the left is the phonon contribution $\eta/s \sim (T/T_F)^{-8}$ deep in the superfluid, the *solid red line* on the right the classical limit $\eta(T) \sim T^{3/2}$ divided by the associated entropy from the Sackur-Tetrode formula. The *red* diamond indicates $T_c \simeq 0.15T_F$. (From Ref. [123])

motivation to search for gravity-duals of non-relativistic, conformally invariant theories, currently an active subject in field theory [116, 117].

In the high-temperature limit $T \gg T_F$, the transport properties of the unitary gas may be described in terms of a Boltzmann equation, which predicts a power law $\eta(T) \sim T^{3/2}$ for the shear viscosity at unitarity [118]. This power law dependence, including the theoretical prediction for the associated prefactor, has recently been verified in the temperature range between T_F and about $7T_F$ by measuring the expansion dynamics of an anisotropic gas released from an optical trap [119], thus extending earlier measurements of η based on the damping of the radial breathing mode [120]. Extraction of the viscosity from the 'elliptic' flow that appears in the transverse expansion from a deformed trap is discussed in detail in the contribution by Schäfer and Chafin to this volume. At low temperatures, in the superfluid regime, a finite viscosity arises from the presence of a normal fluid component. Asymptotically, phonon-phonon collisions dominate, giving rise to a rapid increase $\eta(T) \sim T^{-5}$ of the viscosity as the temperature approaches zero [121]. In fact, this behavior is completely analogous to that of superfluid ^{4}He, a problem that had been solved by Landau and Khalatnikov in 1949 [122]. Unfortunately, the superfluid regime and the expected rise in η have so far not been accessible experimentally. It is certain, however, that both the viscosity and the ratio η/s of the unitary gas necessarily exhibit a minimum, a behavior, which is in fact typical for any fluid [114]. Quantitative predictions for the viscosity of the unitary gas down to the superfluid transition temperature have been obtained recently by Enss et al. [123]. They are based on a diagrammatic evaluation of the exact Kubo-formula within a Luttinger-Ward approach. The formalism respects all symmetries of the problem, in particular scale invariance, and thus gives a vanishing bulk viscosity. Moreoever, it also obeys an exact sum rule for the frequency dependent shear viscosity $\eta(\omega)$ derived by Taylor and Randeria [65].

The sum rule implies that $\eta(\omega)$ decays like $\sim C_\eta/\sqrt{\omega}$ at large frequencies with a prefactor C_η that is proportional to the Tan contact density C. The ratio η/s of the unitary gas is shown in Fig. 1.4. It exhibits a shallow minimum just above the critical temperature of the superfluid transition. The associated value $\eta/s \simeq 0.6\hbar/k_B$ is a factor of about seven above the KSS bound, slightly larger than that found for the relativistic quark-gluon plasma [114]. The unitary gas in fact appears to be the most perfect of all *non*-relativistic fluids known so far!

A closely related issue is the behavior of shear- and spin-diffusion of a scale invariant fluid. Indeed, as was shown by Hohenberg and Martin [90], there is a simple Einstein relation $\eta = \rho_n D_\eta$ that connects the shear viscosity η to the shear diffusion constant D_η via the normal fluid mass density ρ_n. The minimum value $\eta \simeq 0.5\hbar n$ of the shear viscosity in the normal state just above the superfluid transition [123] thus implies that the shear diffusion constant has a minimum value $D_\eta \simeq 0.5\hbar/m$ that only depends on fundamental constants. A similar result has been found recently in an experiment which measures the spin diffusion constant D_s from the equilibration dynamics of two initally separated spin components of the unitary gas [124]. This diffusion constant is related to a spin conductivity σ_s by an Einstein relation of the form $D_s = \sigma_s/\chi_s$, where χ_s is the equilibrium spin-susceptibility. At temperatures close to, but still above, the superfluid transition, D_s attains a minimum value $D_s \simeq 6.3\hbar/m$ [124].

1.7 RF Spectroscopy: Pairing Gap and Pseudogap

Atomic gases offer many internal (hyperfine) states. Superfluid mixtures are prepared in two of these, which are labeled "up" and "down" or $|1\rangle$ and $|2\rangle$, while all other internal states are empty. A radiofrequency pulse, properly tuned to the energy difference between an occupied and an empty state, say state $|3\rangle$, can transfer atoms among internal states. For a single atom or a non-interacting collection of atoms, these internal transition frequencies are known with the precision of atomic clocks—in fact, atomic clocks probe such a hyperfine transition in cesium to keep our standard of time. However, if the atom in the initial state, say $|2\rangle$ interacts with other atoms in $|1\rangle$, for example forming a molecular bound state, the rf photon has to first supply the binding energy of the molecule before it can break the bond and transfer the atom from state $|2\rangle$ to state $|3\rangle$. Even in the absence of molecular binding, the atom experiences an energy shift as it interacts with the surrounding gas, and the RF pulse will have to be detuned by the difference in energy shifts between the final and intial state. In atomic clocks, such density-dependent interaction shifts are a major source of systematic error and are thus called clock shifts.

RF spectroscopy has given access to microscopic information on the strongly interacting gas in the BEC-BCS crossover. Initial experiments traced the evolution of the molecular spectrum all the way across resonance [125]. Although two-body physics no longer supports a bound state beyond the resonance, the spectra were still shifted and broad. However, interpretation of the spectra was made difficult by the

fact that the final state $|3\rangle$ employed in these experiments was still strongly interacting with atoms in state $|1\rangle$. In addition, the averaging over the inhomogeneous density in a trap and the associated spatial variation of the fermionic excitation gap Δ did not allow to measure Δ directly. These problems were avoided in experiments that employed locally resolved and 3D reconstructed rf spectroscopy [126]. Working with a $|1\rangle - |3\rangle$ mixture and a rf-transfer to state $|2\rangle$ moreover allowed to essentially eliminate the final state effects [127]. In this manner, the pairing gap $\Delta = 0.44 \pm 0.02\varepsilon_F$ of the unitary gas was measured by injecting unpaired atoms into the superfluid in a slightly imbalanced Fermi mixture [93]. Paired and unpaired atoms responded at different frequencies, allowing to read off the pairing gap.

Detailed information about the excitation spectrum of strongly interacting Fermi gases is provided by momentum resolved rf spectroscopy, first realized by the JILA group [128]. This is the cold atom analog of angle-resolved photoemission spectroscopy (ARPES) [129, 130], one of the most powerful probes of correlated electrons in solid-state materials. The energy and momentum of the excitation are deduced by measuring energy and momentum of the outcoupled atoms, similar to the situation in an ARPES experiment which determines both the energy and momentum of the outgoing electrons. On a microscopic level, the information gained by such an experiment is the occupied or 'hole' part $A_-(\mathbf{k}, \varepsilon)$ of the full single-particle spectral function $A(\mathbf{k}, \varepsilon)$ of the initial, strongly correlated state [16, 108, 131]. The function $A_-(\mathbf{k}, \varepsilon)$, which is just the Fermi function times the $A(\mathbf{k}, \varepsilon)$, has a rather simple physical interpretation: it is the probability density for removing a particle with given momentum $\mathbf{k}$ in the many-body system with an energy ε. For free particles and at zero temperature, therefore, $A_-(\mathbf{k}, \varepsilon) = \delta(\varepsilon - \varepsilon_k)$ for $\varepsilon_k = \hbar^2 k^2/2m < \mu$ while it vanishes for $\varepsilon_k > \mu$. The spectral function thus directly reveals the energy-momentum relationship of a fermionic excitation in the many-body system, including the appearance of an energy gap. The rf spectrum $I(\omega) \sim \sum_k A_-(\mathbf{k}, \varepsilon_\mathbf{k} - \hbar\omega)$ then follows by integrating over all possible momenta of the outgoing atom.

We expect that the hole spectral function in the $T = 0$ superfluid state has a sharp peak

$$A_-(\mathbf{k}, \varepsilon) = Z_\mathbf{k} \delta(\varepsilon - E_\mathbf{k}^{(-)}) \tag{1.8}$$

at an energy

$$E_\mathbf{k}^{(-)} = \mu - \sqrt{\left(\hbar^2 k^2/2m^* - \widetilde{\mu}\right)^2 + \Delta^2} \tag{1.9}$$

with a weight $Z_\mathbf{k}$ and renormalized dispersion similar in form to the usual Bogoliubov quasiparticles with gap Δ. In the Leggett-BCS mean field theory of the crossover, the parameter $m^* = m$, the bare fermion mass, and $\widetilde{\mu} = \mu$, the chemical potential, with the weight $Z_\mathbf{k} = v_\mathbf{k}^2$, the occupation number. Thus the minimum in the dispersion is at $k_\mu = \sqrt{2m\mu}/\hbar$ for $\mu > 0$ (and $k = 0$ for $\mu < 0$) within MFT. Note that, in contrast to the normal state, the fact that v_k^2 is nonzero at *arbitrary* momentum in the superfluid state, gives a finite probability to create a hole even for momenta above k_μ. Moreover, due to the sum over final momenta, the sharp onset of the rf-spectrum in the $T = 0$

MFT appears at $\hbar\omega_{\min} = \sqrt{\mu^2 + \Delta^2} - \mu$, and not at the energy gap scale. In fact, in the BCS limit $\hbar\omega_{\min} \simeq \Delta^2/2\mu$, the condensation energy per particle, which is much less than the gap. Beyond the crossover MFT, interaction effects lead to [16, 83, 92] $\widetilde{\mu} = \mu - U$, shifted away from the chemical potential, and $m^* \neq m$. The predicted negative shift in $\widetilde{\mu}$ of $U \simeq -0.43\varepsilon_F$ at unitarity has been seen in the rf experiments [93].

An important question is whether the energy gap, or more precisely, a strong suppression of spectral weight near the chemical potential, called the pseudogap, persists above T_c in the unitary regime. In this context, a crucial parameter is the crossover temperature scale $T^\star$ (see Fig. 1.1), below which pairing correlations become manifest [39–41]. In the BCS limit, $T^\star$ coincides with T_c, so that the formation of pairs and their condensation occur simultaneously. In the opposite extreme, the BEC limit, $T^\star$ is the temperature scale for molecular dissociation, which is much larger than the Bose condensation T_c. The key quantitative issue near unitarity is the extent of the temparature window $T_c < T < T^\star$, in which various anomalies in spectroscopy and thermodynamics, arising from pairing correlations above T_c, are predicted [39–41]. Since $T^\star$ is a crossover scale, its estimate depends on the observable being probed, in marked contrast with a phase transition. Early estimates [24] and quantum Monte Carlo calculations [132, 133] indicate that $T^\star$ is roughly $0.5T_F$ for the unitary gas, which is about three times T_c. Other theoretical approaches, discussed below, suggest a much smaller window of temperatures [16] at unitarity, though these effects can only increase as one moves to the BEC side. The experiments at present are also not unequivocal on the extent of the temperature range or the size of the pseudogap anomalies. The extent to which both theory and experiment provide clear evidence for the existence of a well-defined a pseudogap regime in the unitary gas is a subject of current debate, as we discuss next.

We first discuss angle-resolved rf spectroscopy above T_c. At a phenomenological level [39, 134], one expects the spectral function in the pseudogap regime to still show an energy gap, and a bending-back of the dispersion (analogous to the Bogoliubov dispersion in the superfluid state) as in Eq. 1.9. This arises because of the persistence of pairing correlations, or 'preformed pairs', above T_c. However, the sharp peak in Eq. 1.8 will be greatly broadened, because one expects quasiparticles to be quite ill-defined in this strongly interacting regime. The very short mean free path, or equivalently short lifetime of fermionic excitations, is closely related to the anomalously low shear viscosity $\eta \simeq 0.5\hbar n$ of the unitary gas in the regime just above T_c discussed in the previous section.

Gap-like features and the associated back-bending of the dispersion *near* k_F have been observed in a recent angle-resolved rf experiment [135]. Note that back-bending *far from* k_F, with small but non-zero spectral weight, is predicted to be a universal feature [109] of Fermi gases with contact interactions in all phases, normal and superfluid. This is a direct consequence of the $1/k^4$-tail in the momentum distribution discussed in Sect. 1.5 This is indeed what the experiments [135] find, with the back-bending at large momenta persisting up to very high T, even when the near-k_F behavior no longer exhbits a pseudogap. A quantitative estimate of the energy gap, either the pseudogap above T_c or the superconducting gap below T_c, requires

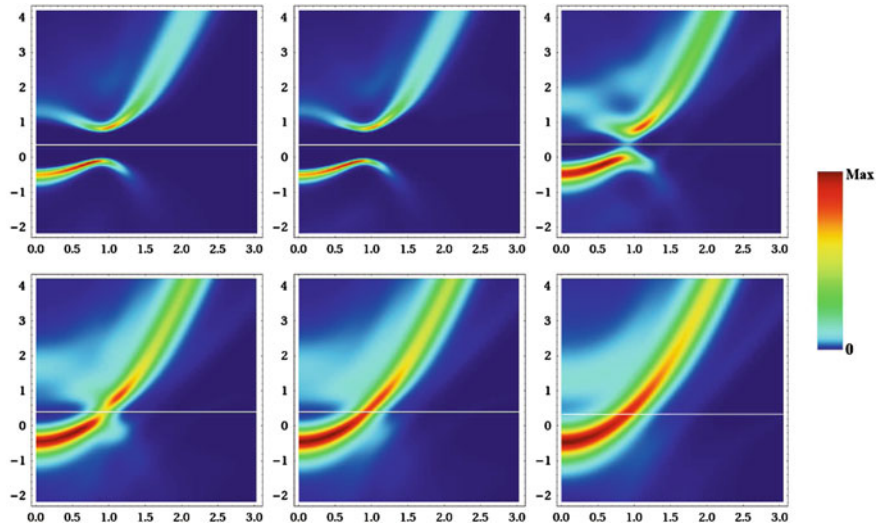

Fig. 1.5 Density plots of the spectral function $A(\mathbf{k}, \varepsilon)$ at unitarity for different temperatures. Momentum and energy are in units of k_F or ε_F respectively. From top left to bottom right: $T/T_F = 0.01,\ 0.06,\ 0.14,\ 0.160(T_c), 0.18, 0.30$. The white horizontal lines mark the chemical potential μ (From [16])

measuring the near k_F feature with respect to the chemical potential. Eventually, such measurements could help to answer the question whether or not sharp quasiparticle excitations exist in the normal fluid regime above T_c.

The contributions by Strinati and by Bulgac, Forbes and Magierski, describe two different microscopic approaches—the pair-fluctuation approach to the BCS–BEC crossover [108, 131, 136] and quantum Monte Carlo calculations [133], respectively—both of which lead to characteristic pseudogap spectral features.

The full spectral functions of the unitary gas as a function of momentum and energy for temperatures across the superfluid transition as obtained from the Luttinger-Ward approach [16] is shown in Fig. 1.5. Deep in the superfluid state, the dispersion of both the hole (below μ) and particle branch (above μ) exhibits a BCS-Bogoliubov-like dispersion, as expected from Eq. 1.9. The shift of $\widetilde{\mu}$ from the chemical potential by the interaction-induced shift $U \simeq -0.46\varepsilon_F$. is also observed. With increasing temperature the gap closes and the two branches gradually merge. Apparently, in this approach, the backbending very quickly disappears above $T_c \simeq 0.16T_F$ and there is no pronounced pseudogap regime.

Pairing corelations above T_c are also of relevance in understanding the thermodynamics of the BCS–BEC crossover in the normal state. It was predicted [40, 41] in early calculations of two dimensional lattice models of the BCS–BEC crossover that in the temperature range $T_c < T < T^\star$ (see Fig. 1.1), there is a strong suppression of the spin susceptibility χ_s with lowering T, while the compressibility $dn/d\mu$ is T-independent. This qualitative difference between the behaviors of χ_s and $dn/d\mu$

represent a marked deviation from conventional Fermi liquid behavior in a strongly interacting, degenerate Fermi system. Whether these effects are significant in the three dimensional continuum problem at unitarity depends on the separation between T_c and $T^\star$, as already noted.

The expected strong reduction of the spin susceptibility below $T^\star$ due to the formation of singlet pairs can, in principle, be measured with ultracold atoms by observing the displacement of the two spin-components induced by a trapping potential which acts differently on both hyperfine states [137]. In practice, unfortunately, this is difficult because in the case of ^{6}Li, the polarizabilities are essentially equal at the magnetic fields of interest. A quite different method to determine the spin susceptibility has opened up recently with the measurement of the spin diffusion constant D_s mentioned above. Indeed, an independent mesasurement of D_s and the associated spin conductivity σ_s allows to extract the equilibrium spin susceptibility $\chi_s = \sigma_s / D_s$ as their ratio. The resulting $\chi_s(T)$ of the unitary gas shows no clear suppression in the regime above the superfluid transition, indicating that the characteristic temperature $T^\star$ may not be much higher than T_c at unitarity.

To conclude this section, it seems appropriate to point out similarities and differences between the pairing pseudogap in the BCS–BEC crossover and the much discussed—but still not well understood—pseudogap phase in underdoped high-T superconductors. In fact, the early work [39–41] on pseudogaps in the crossover problem was motivated by the desire to see if the normal state of a short coherence length superconductor, with pair size comparable to interparticle distance, might generically show deviations from Fermi liquid behavior. As emphasized in the introduction, the high Tc superconductors (HTSC) differ from the ultracold Fermi gases in essential microscopic details. In the HTSC the electrons live in the two-dimensional copper-oxygen planes of a highly anisotropic crystal, and the dominant interactions arise from Coulomb repulsion. *d*-wave pairing and superconductivity arises upon doping—i.e., adding mobile carriers to—a parent antiferromagnetic Mott insulator. The superfluid phase competes with a variety of different order parameters, including antiferromagnetism and charge ordering. By contrast, the neutral atoms in a Fermi gas have manifestly attractive interactions, the only instability is to s-wave pairing and the superfluid state is free from competing order parameters or a proximity to a Mott transition.

Despite these differences, there are insights from the much better understood problem of the BCS–BEC crossover that may be useful for the HTSC cuprates. In both systems one can be in strong interaction regimes where (1) the pair size is comparable to interparticle spacing, (2) a simple mean-field description of the phase transition fails, and (3) T_c is determined by the superfluid stiffness rather than the pairing gap. In the underdoped cuprates, that lie between the highest T_c optimally doped superconductor and the parent Mott Insulator, there is clear evidence for a normal state pseudogap [23]. The associated loss of spectral weight above T_c has a strong angular anisotropy revealed by ARPES measurements [129, 130]. Although there are striking similarities between the anisotropy of the pseudogap above T_c and the *d*-wave superconducting gap below T_c, the connection between the two gaps gap remains controversial. The pseudogap regime in the HTSC exhibits features arising

from competing order parameters, local pairing above T_c, and proximity to the Mott insulator. The problem of the unitary Fermi gas, in turn, is in many ways simpler with a single instability to s-wave pairing. Thus if a gap exists above T_c, it can only be related to precursor pairing correlations.

1.8 Spin Imbalance and the Fermi Polaron

In standard BCS theory, pairs are formed in an s-wave state between fermions with opposite spins. The question of what happens if not every spin up fermion can find a spin down partner has intrigued physicists ever since the early days of BCS theory. In conventional superconductors, unequal populations of up and down-spin electrons are very difficult to create, essentially because superconductivity is destroyed by the orbital effects in the presence of a magnetic field long before the Zeeman splitting is able to induce an appreciable imbalance. In an early study, however, Chandrasekhar and Clogston independently considered what would be the maximum critical field if it enters a superconductor at all and no orbital effects were present [138, 139]. Such a field would imbalance the chemical potentials of spin up and spin down electrons by the Zeeman energy $\pm\mu_B B$, where μ_B is Bohr's magneton. Eventually, it would be energetically more favorable to form an imbalanced normal state than to force atoms with vastly different Fermi energies to pair up. The critical field is reached when the Zeeman energy overcomes the pairing gap, $\mu_B B > \Delta/\sqrt{2}$. In the weak coupling limit, where $2\Delta = 3.52\, k_B T_c$, this gives $B = 18.5$ Tesla for $T_c = 10$ K. Conventional superconductors do not reach such high critical fields, but heavy fermion superconductors [8, 140] or layered organic superconductors [141] may be in this "Pauli limited" regime.

In atomic gases, the population imbalance can be chosen at will. In fact, imbalance is yet another way, besides increasing the temperature or reducing the scattering length, to probe how stable the superfluid is. A detailed discussion of the present state of knowledge about the set of questions associated with imbalanced gases is given in the contributions by Chevy and Salomon from an experimental and by Diederix and Stoof as well as by Recati and Stringari from a theoretical perspective. It turns out, that there is a critical value of the imbalance beyond which the superfluid turns into a normal Fermi liquid. For the homogeneous unitary gas, the critical imbalance $\sigma_c = (n_\uparrow - n_\downarrow)/(n_\uparrow + n_\downarrow) \simeq 0.4$ in the ground state has been determined from quantum Monte Carlo calculations by comparing the energy of the balanced superfluid with that of an imbalanced normal state [142]. The superfluid-to-normal transition at $T = 0$ is, to current knowledge, first order in nature as long as $1/k_F a$ is less than a critical value close to 0.8 [16]. This is the location of the splitting point mentioned in the introduction. Beyond this point, on the BEC-side, single Fermions can be added to a balanced superfluid in a continuous manner. With increasing imbalance the system thus stays superfluid, effectively as a Bose-Fermi mixture up until full polarization, where the gas is a trivial non-interacting Fermi gas. The breakdown of superfluidity with increasing imbalance in a trap has been measured by observing the disappearance of a vortex lattice [143]. As shown in Fig. 1.6, for

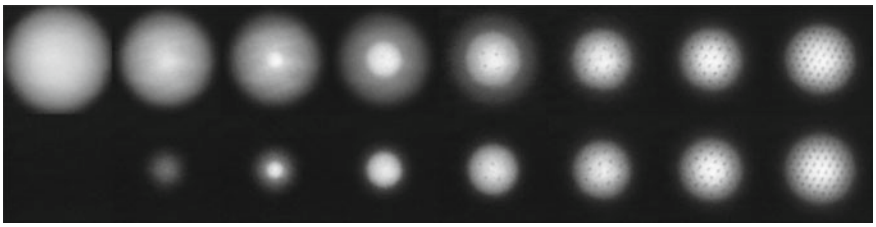

Fig. 1.6 Observation of vortices in a strongly interacting Fermi gas with imbalanced spin populations. The population imbalance $(N_\uparrow - N_\downarrow)/(N_\uparrow + N_\downarrow)$ was (from left to right) 100, 90, 80, 62, 28, 18, 10 and 0%. From [143]

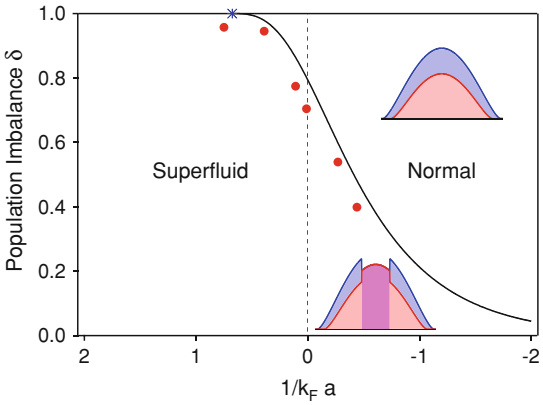

Fig. 1.7 Critical population imbalance $\delta = (N_\uparrow - N_\downarrow)/(N_\uparrow + N_\downarrow)$ between the two spin states for which the superfluid-to-normal transition is observed. The profiles indicate the distribution of the gas in the harmonic trap. Data from [143]

the unitary gas superfluidity breaks down beyond a ratio of 85%/15% between the two spin states.

Since vortices are difficult to create and observe near the phase boundaries, the superfluid phase diagram has also been mapped out by using pair condensation as an indicator for superfluidity. The resulting phase diagram is shown in Fig. 1.7. As was mentioned above, on the BEC side the critical value of the imbalance where superfluidity is destroyed by the Chandrasekhar-Clogston mechanism of a mismatched Fermi sphere between the two components approaches 100%. This can be understood by noting that in this regime even a tiny concentration of minority atoms in a majority Fermi sea will form bosonic molecules with the majority atoms, which then give rise to a Bose-Einstein condensate.

The first order transition between the superfluid at equal spin population and the imbalanced normal mixture gives rise to phase separation. First hints for phase separation between the normal and superfluid phase were seen in Refs. [72, 143, 144]. Using tomographic techniques, a sharp separation between a superfluid core and a partially polarized normal phase was found [145] (see Fig. 1.8). Finally, the phase diagram of a spin-polarized Fermi gas at unitarity was obtained, by mapping out the superfluid phase versus temperature and density imbalance [146]. Using tomo-

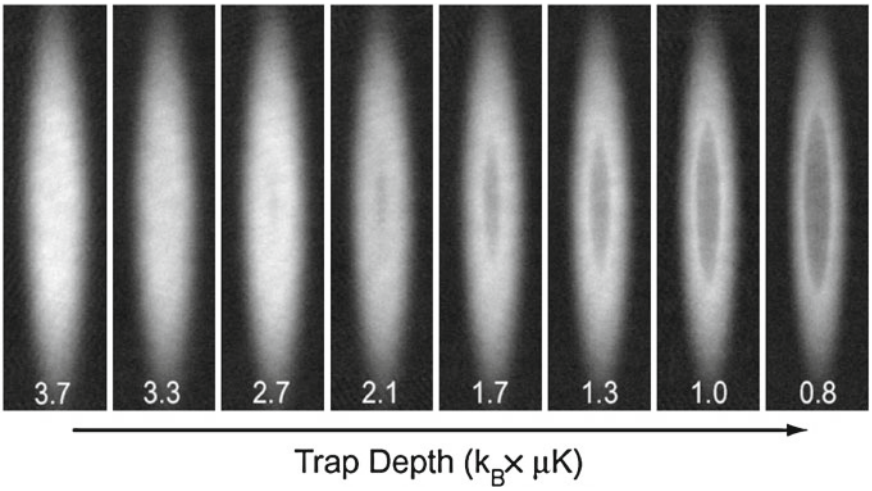

Fig. 1.8 Direct observation of the phase transition in imbalanced gases. The images are of the column density difference between spin up and spin down atoms. Below a critical temperature, an "empty" core opens up, signalling superfluid pairing at equal densities [145]

graphic techniques, spatial discontinuities in the spin polarization were revealed. This is the signature of a first-order phase transition which disappears at a tricritical point, in agreement with theoretical predictions [142, 147]. A detailed discussion of the structure of the phase diagram of the imbalanced unitary gas is given in the contributions by Diederix and Stoof and by Recati and Stringari.

While a detailed understanding of whether imbalanced Fermi gases with strong attractive interactions exhibit more complex phases than a normal Fermi liquid or a mixed superfluid/normal Fermi gas is still missing (see section 9 below and the contributions by Bulgac, Forbes and Magierski for a discussion of possible exotic phases in this context), considerable progress has been made within the last few years in the limit of a very large imbalance. In this limit, the two component Fermi gas can be viewed as a small number of spin down, minority impurities swimming in a Fermi sea of spin up particles. For a weakly-attractive interaction between the impurity and the Fermi sea, the impurity propagates freely through the medium, experiencing only a mean field energy shift $4\pi\hbar^2 a n_\uparrow / m$ from forward-scattering, where n is the majority density, a the scattering length between spin up and spin down. However, as interactions increase and the mean free path becomes comparable to the interparticle distance, momentum changing collisions become important. In the strong coupling regime, the impurity dresses itself with a polarization cloud of majority atoms, giving rise to a new type of quasiparticle: the Fermi polaron. The question of whether a single added down-spin behaves like a proper quasiparticle can be addressed by calculating the quasiparticle residue, the probability that an added bare particle with momentum $\mathbf{p}$ will propagate with this very momentum for an arbitrary long time [148, 149]. For very strong attraction, this picture is expected to break down: Here, an added

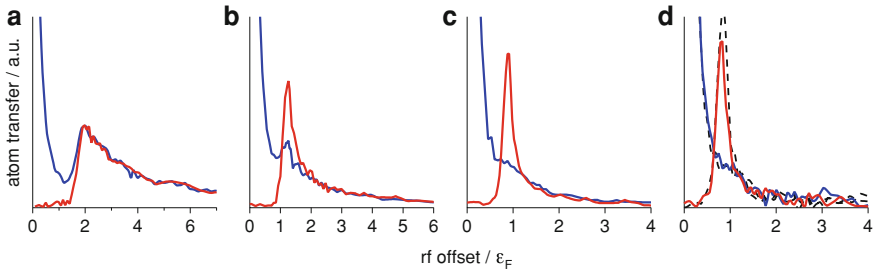

Fig. 1.9 RF spectroscopy on polarons. Shown are spatially resolved, 3D reconstructed rf spectra of the environment (*blue*, state $|1\rangle$) and impurity (*red*, state $|3\rangle$) component in a highly imbalanced spin-mixture. **a** Molecular limit. **b**, **c** Emergence of the polaron, a distinct peak exclusively in the minority component. **d** At unitarity, the peak dominates the impurity spectrum. For the spectra shown as dashed lines in **d** the roles of states $|1\rangle$ and $|3\rangle$ are exchanged. Impurity concentration was $x = 5(2)\%$ for all spectra, the interaction strengths $1/k_F a$ were **a** 0.76(*2*), **b** 0.43(*1*) c) 0.20(*1*), d) 0 (Unitarity)

down-spin will form a spin-zero, mobile molecular bound state with the up-spin Fermi sea. The fermionic quasiparticle will therefore vanish beyond a critical value of the coupling $1/(k_{F\uparrow}a)$, via a discontiuous transition first predicted by Prokof'ev and Svistunov [150].

Polarons have been observed via locally resolved RF spectroscopy [151]. In the case of molecular binding, one finds the characteristic onset at the molecular binding energy, and fully coincidal spectra for both the spin up and spin down atoms-as binding is a purely two-body affair. For the polaron, a characteristic bimodal spectrum is observed: A narrow, coherent quasi-particle peak, centered at the polaron binding energy, which emerges from a broad, incoherent background (see Fig. 1.9).

The results for the ground state energy of the Fermi polaron are in quite good agreement with the result of a variational Ansatz for the ground state wave function due to Chevy, in which the single down spin is dressed with particle-hole excitations of the up-spin Fermi sea [152, 153]. This approximate treatment is supported by a more detailed analysis including multiple particle-hole pairs [154], and also by Quantum Monte-Carlo calculations [150, 155]. The effective mass of Fermi polarons at unitarity has been deduced from density profiles [156]. As discssed in the contributions by Chevy and Salomon and by Recati and Stringari, it can be determined in a direct manner from a dynamical measurement, by extrapolating frequencies of collective excitations in strongly imbalanced Fermi mixtures to the single-impurity limit [157]. The result of $m^* = 1.20(10)m$ is in good agreement with theoretical predictions [150]. The polaron energy was observed to be largely independent of the impurity density, i.e. interaction effects between the dressed particles must be weak.

At a critical interaction strength $1/(k_{F\uparrow}a) = 0.76$, the Fermi Polaron peak vanishes and a transition towards two-body binding is observed [151]. The disappearance of the Fermi polaron as a spin *1/2* quasiparticle beyond a critical value of the coupling was predicted by diagrammatic Monte Carlo calculations [148, 150]

and was later studied by variational methods [149, 158]. At this point, a Fermi liquid of polarons is replaced by a Bose liquid of molecules. At low enough temperatures, this molecular cloud will form a Bose condensate that fully phase separates from the normal state of unpaired atoms, as observed in [159]. Even further away from the Feshbach resonance, when the interactions between molecules and atoms become weaker, one might be able to observe fermionic atoms moving in a bath of bosons. This would be an example of the "classical" polaron, a fermion (electron) dressed by a boson bath (phonons).

1.9 FFLO Phases and Outlook

A remarkable proposal of what might happen in a fermionic superfluid in the presence of a finite spin-imbalance was put forward almost fifty years ago by Fulde and Ferrell and independently by Larkin and Ovchinnikov [160, 161]. The novel type of superfluidity, now often abbreviated as FFLO or LOFF states, predicts that Cooper pairs acquire a non-vanishing center-of-mass momentum. As a result, the superfluid order parameter exhbits a nontrivial periodic modulation in space, thereby spontaneously breaking translation invariance. Due to the coexistence of fermionic superfluidity and periodic order such a state has also been called a 'Fermi supersolid' [162]. In solid state materials, the orbital effect of an external magnetic field usually overwhelms the Zeeman effect causing spin imbalance. Despite decades of intensive search, there are very few systems in which there is now some indirect experimental evidence for the occurrence of FFLO order: layered organic superconductors with a strong parallel magnetic field [141] and certain heavy fermion materials [8, 140]. A quite different context where superfluid states with additional periodic order might show up are color superfluids that are expected in the core of neutron stars [10]. In this case, the imbalance arises as a result of the different chemical potentials due to different quark masses.

As disussed in the previous section, ultracold atoms provide an ideal model system to study attractive Fermi gases with an adjustable value of the spin-imbalance. For a Fermi gas near unitarity, one expects in fact that for small imbalances the ground state exhibits FFLO order. This conclusion is supported both on general grounds [17] and also on a generalization of density functional theory that includes superfluid ordering and a finite spin imbalance, as discussed in the contribution by Bulgac et al. Unfortunately, in the 3D case, neither the precise type of spatial order, nor the relevant range of stability of an FFLO phase with respect to temperature are known. In addition, the inhomogeneous density in the trap leads to a situation where an FFLO phase would appear sandwiched between a balanced superfluid in the center and a polarized normal phase around it. This makes an observation very difficult if not impossible. As is discussed in detail in the contribution by Feiguin et al. the situation is much more promising in a one-dimensional configuration for two reasons: First of all, it turns out that in one dimension and for negative 3D scattering lengths (i.e. essentially on the BCS-side of the crossover) the ground state of the attractive

Fermi gas exhibits FFLO order at *arbitrary* values of the polarization. As a second point, in contrast to the 3D case, the interesting phase with finite imbalance appears in the center of the trap and not in its wings. From a theory point of view, the 1D case has the additional advantage that a number of exact results are available through the Bethe-Ansatz. For instance, a complete analytic solution can be given for the BCS–BEC crossover of the balanced gas [163, 164]. Moreover, efficient numerical methods like the density matrix renormalization group allow to obtain quantitatively reliable results for realistic system sizes without the Fermionic sign problem.

Experimentally, attractive Fermi gases confined in 1D tubes have been realized by the Rice group [165]. The observed spin-resolved density profiles show the predicted phase separation into an imbalanced gas in the center and a balanced superfluid at the edge of the trap. Unfortuately, so far experiments have not demonstrated that the phase in the center of the trap indeed corresponds to a paired state with FFLO order. This is not a trivial task and requires e.g. to resolve spin density modulations on a rather small length scale or a time-of-flight measurement that reveals the momentum distribution of the pairs. Due to their finite center-of-mass momentum, peaks should appear at a nonzero momenta $\pm Q$ with Q increasing linearly with the imbalance.

As a result of a breathtaking sequence of experiments and new theoretical insights over a short period of time, ultracold Fermi gases have developed into an exciting new form of matter with unexpected properties. The realization of the BEC-BCS crossover, the observation of vortex lattices in neutral fermionic superfluids and precision measurements of universal numbers in the thermodynamics of the unitary Fermi gas have come alongside with new theoretical concepts like the ε-expansion for scale invariant many-body systems, the Tan relations or the Fermi polaron as a novel type of a quantum impurity problem. Unconventional superfluids like the FFLO phase or a quite subtle liquid of trions in a mixture of three-component Fermi gases [166, 167] that resembles the hadrons of QCD [168] appear in reach within the coming years. Ultracold Fermi gases present us with a model textbook system, that did not exist before, with simple and controllable interactions, dimensionality and spin composition. Eventually, the goal is to deepen our understanding of fermions, the building blocks of matter, in the presence of strong interactions. The field has taken the first important steps, but this is only the beginning.

Acknowledgments M.R. would like to thank the US National Science Foundation (NSF-DMR 0706203) and the US Army Research Office (ARO W911NF- 08-1-0338) for support. W.Z. acknowledges support from the Deutsche Forschungsgemeinschaft through FOR801.

References

1. Regal, C.A., Greiner, M., Jin, D.S.: Phys. Rev. Lett. **92**, 040403 (2004)
2. Zwierlein, M., Stan, C., Schunck, C., Raupach, S., Kerman, A., Ketterle, W.: Phys. Rev. Lett. **92**, 120403 (2004)
3. Bardeen, J., Cooper, L.N., Schrieffer, J.R.: Phys. Rev. **108**, 1175 (1957)
4. Tinkham, M.: Introduction to Superconductivity, 2nd edn. Dover, Mineola (2004)

5. Bohr, A., Mottelson, B.R., Pines, D.: Phys. Rev. **110**, 936 (1958)
6. Migdal, A.B.: Nucl. Phys. **13**, 655–674 (1959)
7. Vollhardt, D., Wölfle, P.: The Superfluid Phases of Helium 3. Taylor and Francis, London (1990)
8. Pfleiderer, C.: Rev. Mod. Phys. **81**, 1551 (2009)
9. Mackenzie, A.P., Maeno, Y.: Rev. Mod. Phys. **75**, 657 (2003)
10. Alford, M.G., Schmitt, A., Rajagopal, K., Schäfer, T.: Rev. Mod. Phys. **80**, 1455–1461 (2008)
11. Schafroth, M.R., Butler, S., Blatt, J.: Helv. Phys. Acta **30**, 93 (1957)
12. Schafroth, M.R.: Phys. Rev. **111**, 72 (1958)
13. Griffin, A., Snoke, D., Stringari, S.: Bose-Einstein Condensation. Cambridge University Press, Cambridge (1995)
14. Eagles, D.M.: Phys. Rev. **186**, 456 (1969)
15. Leggett, A.: Diatomic molecules and Cooper pairs. In: Modern Trends in the Theory of Condensed Matter. Proceedings of the XVIth Karpacz Winter School of Theoretical Physics, Karpacz, Poland, Springer, Berlin 13–27 (1980)
16. Haussmann, R., Punk, M., Zwerger, W.: Phys. Rev. A **80**, 063612 (2009)
17. Son, D., Stephanov, M.: Phys. Rev. A **74**, 013614 (2006)
18. Klinkhamer, F.R., Volovik, G.E.: JETP Lett. **80**, 343 (2004)
19. Randeria, M., Duan, J., Shieh, L.: Phys. Rev. B **41**, 327 (1990)
20. Read, N., Dmitry Green, D.: Phys. Rev. B **97**, 10267 (2000)
21. Nozières, P., Schmitt-Rink, S.: J. Low Temp. Phys. **59**, 195–211 (1985)
22. Randeria M.: Crossover from BCS theory to Bose-Einstein condensation. In: Griffin, A., Snoke, D., Stringari, S. (eds.) Bose-Einstein Condensation. Cambridge University Press, Cambridge 355– 392 (1995)
23. Lee, P.A., Nagaosa, N., Wen, X.-G.: Rev. Mod. Phys. **78**, 17 (2006)
24. Sade Melo, C.A.R., Randeria, M., Engelbrecht, J.R.: Phys. Rev. Lett. **71**, 3202 (1993)
25. Randeria, M.: Nature Phys. **6**, 561 (2010)
26. Engelbrecht, J.R., Randeria, M., Sade Melo, C.A.R.: Phys. Rev. B **55**, 15153 (1997)
27. Drechsler, M., Zwerger, W.: Annalen der Physik **1**, 15–23 (1992)
28. Randeria, M., Duan, J.-M., Shieh, L.: Phys. Rev. Lett. **62**, 981 (1989)
29. Petrov, D., Salomon, C., Shlyapnikov, G.: Phys. Rev. Lett. **93**, 090404 (2004)
30. Mora, C., Komnik, A., Egger, R., Gogolin, A.O.: Phys. Rev. Lett. **95**, 080403 (2005)
31. Petrov, D.S., Baranov, M.A., Shlyapnikov, G.V.: Phys. Rev. A **67**, 031601 (2003)
32. Haussmann, R.: Phys. Rev. B **49**, 12975 (1994)
33. Haussmann, R., Rantner, W., Cerrito, S., Zwerger, W.: Phys. Rev. A **75**, 023610 (2007)
34. Nishida, Y., Son, D.T.: Phys. Rev. Lett. **97**, 050403 (2006)
35. Nishida, Y., Son, D.T.: Phys. Rev. A **75**, 063617–22 (2007)
36. Burovski, E., Prokof'ev, N., Svistunov, B., Troyer, M.: Phys. Rev. Lett. **96**, 160402 (2006)
37. Burovski, E., Kozic, E., Prokof'ev, N., Svistunov, B., Troyer, M.: Phys. Rev. Lett. **101**, 090402 (2008)
38. Goulko, O., Wingate, M.: Phys. Rev. A **82**, 053621 (2010)
39. Randeria M.: Precursor pairing correlations and pseudogaps. In: Iadonisi, G., Schrieffer, J.R., Chiafalo, M.L. (eds.) Proceedings of the International School of Physics "Enrico Fermi" Course CXXXVI on High Temperature Superconductors. IOS Press, Amsterdam 53–75 (1998)
40. Randeria, M., Trivedi, N., Moreo, A., Scalettar, R.T.: Phys. Rev. Lett. **69**, 2001 (1992)
41. Trivedi, N., Randeria, M.: Phys. Rev. Lett. **75**, 312 (1995)
42. Bertsch G.: Proceedings of the tenth international conference on recent progress in many-body theories. In: Bishop, R., Gernoth, K.A., Walet, N.R., Xian, Y. (eds.) Recent Progress in Many-Body Theories. World Scientific, Seattle (2000)
43. Baker, G.A.: Phys. Rev. C **60**, 054311 (1999)
44. Schwenk, A., Pethick, C.J.: Phys. Rev. Lett. **95**, 160401 (2005)
45. DeMarco, B., Jin, D.: Science **285**, 1703–1706 (1999)

46. Granade, S.R., Gehm, M.E., O'Hara, K.M., Thomas, J.E.: Phys. Rev. Lett. **88**, 120405 (2002)
47. Hadzibabic, Z., Stan, C.A., Dieckmann, K., Gupta, S., Zwierlein, M., Grlitz, A., Ketterle, W.: Phys. Rev. Lett. **88**, 160401 (2002)
48. Roati, G., Riboli, F., Modugno, G., Inguscio, M.: Phys. Rev. Lett. **89**, 150403 (2002)
49. Schreck, F., Khaykovich, L., Corwin, K.L., Ferrari, G., Bourdel, T., Cubizolles, J., Salomon, C.: Phys. Rev. Lett. **87**, 080403 (2001)
50. Truscott, A.G., Strecker, K.E., McAlexander, W.I., Partridge, G.B., Hulet, R.G.: Science **291**, 2570–2572 (2001)
51. Courteille, P., Freeland, R., Heinzen, D., van Abeelen, F., Verhaar, B.: Phys. Rev. Lett. **81**, 69–72 (1998)
52. Inouye, S., Andrews, M.R., Stenger, J., Miesner, H.J., Stamper-Kurn, D.M., Ketterle, W.: Nature **392**, 151–154 (1998)
53. Chin, C., Grimm, R., Julienne, P., Tiesinga, E.: Rev. Mod. Phys. **82**, 1225 (2010)
54. Tiesinga, E., Verhaar, B., Stoof, H.: Phys. Rev. A **47**, 4114–4122 (1993)
55. Bloch, I., Dalibard, J., Zwerger, W.: Rev. Mod. Phys. **80**, 885 (2008)
56. Bruun, G., Pethick, C.: Phys. Rev. Lett. **92**, 140404 (2004)
57. Ketterle W., Zwierlein, M.: Making, probing and understanding ultracold Fermi gases. In: Inguscio, M., Ketterle, W., Salomon, C. (eds.) Ultracold Fermi Gases, Proceedings of the International School of Physics "Enrico Fermi", Course CLXIV, Varenna, 20–30 June 2006. IOS Press, Amsterdam (2008)
58. Nikolic, P., Sachdev, S.: Phys. Rev. A **75**, 033608–0336014 (2007)
59. Nishida, Y., Son, D.T.: Phys. Rev. D **76**, 086004 (2007)
60. Son, D.T., Wingate, M.: Ann. Phys. **321**, 197–224 (2006)
61. Werner, F., Castin, Y.: Phys. Rev. A **74**, 053604 (2006)
62. Pitaevskii, L.P., Rosch, A.: Phys. Rev. A **55**, R853 (1997)
63. Ho, T.-L.: Phys. Rev. Lett. **92**, 090402 (2004)
64. Son, D.T.: Phys. Rev. Lett. **98**, 020604–4 (2007)
65. Taylor, E., Randeria, M.: Phys. Rev. A **81**, 053610 (2010)
66. Bartenstein, M., Altmeyer, A., Riedl, S., Jochim, S., Chin, C., Hecker-Denschlag, J., Grimm, R.: Phys. Rev. Lett. **92**, 120401 (2004)
67. Bourdel, T., Cubizolles, J., Khaykovich, L., Magalh"aes, K.M.F., Kokkelmans, J.M.F., Shlyapnikov, G.V., Salomon, C.: Phys. Rev. Lett. **91**, 020402 (2003)
68. Gehm, M.E., Hemmer, S.L., Granade, S.R., O'Hara, K.M., Thomas, J.E.: Phys. Rev. A **68**, 011401 (2003)
69. O'Hara, K.M., Hemmer, S.L., Gehm, M.E., Granade, S.R., Thomas, J.E.: Science **298**, 2179 (2002)
70. Bourdel, T., Khaykovich, L., Cubizolles, J., Zhang, J., Chevy, F., Teichmann, M., Tarruell, L., Kokkelmans, S., Salomon, C.: Phys. Rev. Lett. **93**, 050401 (2004)
71. Kinast, J., Turlapov, A., Thomas, J.E., Chen, Q., Stajic, J., Levin, K.: Science **307**, 1296–1299 (2005)
72. Partridge, G.B., Li, W., Kamar, R.I., Liao, Y., Hulet, R.G.: Science **311**, 503 (2006)
73. Stewart, J.T., Gaebler, J.P., Regal, C.A., Jin, D.S.: Phys. Rev. Lett. **97**, 220406 (2006)
74. Nascimbène, S., Navon, N., Jiang, K.J., Chevy, F., Salomon, C.: Nature **463**, 1057–1060 (2010)
75. Navon, N., Nascimbene, S., Chevy, F., Salomon, C.: Science **328**, 729 (2010)
76. Heiselberg, H.: Phys. Rev. A **63**, 043606 (2001)
77. Hu, H., Drummond, P.D., Liu, X.-J.: Nat. Phys. **3**, 469–472 (2007)
78. Perali, A., Pieri, P., Strinati, G.C.: Phys. Rev. Lett. **93**, 100404 (2004)
79. Diener, R.B., Sensarma, R., Randeria, M.: Phys. Rev. A **77**, 023626 (2008)
80. Hu, H., Liu, X.-J., Drummond, P.: Europhys. Lett. **74**, 574–580 (2006)
81. Astrakharchik, G.E., Boronat, J., Casulleras, J., Giorgini, S.: Phys. Rev. Lett. **93**, 200404 (2004)

82. Carlson, J., Chang, S.-Y., Pandharipande, V.R., Schmidt, K.E.: Phys. Rev. Lett. **91**, 050401 (2003)
83. Carlson, J., Reddy, S.: Phys. Rev. Lett. **95**, 060401 (2005)
84. Bulgac, A., Drut, J.E., Magierski, P.: Phys. Rev. A **78**, 023625 (2008)
85. Forbes, M.M., Gandolfi, S., Gezerlis, A.: Phys. Rev. Lett. **106**, 235303 (2011)
86. Nussinov, Z., Nussinov, S.: Phys. Rev. A **74**, 053622–053629 (2006)
87. Randeria, M., Duan, J.-M., Shieh, L.-Y.: Phys. Rev. Lett. **62**, 981 (1989)
88. Arnold, P., Drut, J.E., Son, D.T.: Phys. Rev. A **75**, 043605 (2007)
89. Nishida, Y.: Phys. Rev. A **79**, 013627–5 (2009)
90. Hohenberg, P.C., Martin, P.C.: Ann. Phys. **34**, 291–359 (1965)
91. Haussmann, R., Zwerger, W.: Phys. Rev. A **78**, 063602 (2008)
92. Carlson, J., Sanjay, R.: Phys. Rev. Lett. **100**, 150403 (2008)
93. Schirotzek, A., Shin, Y., Schunck, C.H., Ketterle, W.: Phys. Rev. Lett. **101**, 140403 (2008)
94. Gor'kov, L., Melik-Barkhudarov, T.: Zh. Eskp. Theor. Fiz. **40**, 1452 (1961)
95. Heiselberg, H., Pethick, C.J., Smith, H., Viverit, L.: Phys. Rev. Lett. **85**, 2418 (2000)
96. Floerchinger, S., Scherer, M., Diehl, S., Wetterich, C.: Phys. Rev. B **78**, 174528 (2008)
97. Diener, R.B., Randeria, M.: Phys. Rev. A **81**, 033608 (2010)
98. Tan, S.: Ann. Phys. **323**, 2971–2986 (2008)
99. Tan, S.: Ann. Phys. **323**, 2952–2970 (2008)
100. Braaten, E., Platter, L.: Phys. Rev. Lett. **100**, 205301 (2008)
101. Stewart, J.T., Gaebler, J.P., Drake, T.E., Jin, D.S.: Phys. Rev. Lett. **104**, 235301 (2010)
102. Werner, F., Tarruell, L., Castin, Y.: Europ. Phys. J. B **68**, 401–415 (2009)
103. Zhang, S., Leggett, A.J.: Phys. Rev. A **79**, 023601 (2009)
104. Partridge, G.B., Strecker, K.E., Kamar, R.I., Jack, M.W., Hulet, R.G.: Phys. Rev. Lett. **95**, 020404 (2005)
105. Baym, G., Pethick, C.J., Yu, Z., Zwierlein, M.W.: Phys. Rev. Lett. **99**, 190407 (2007)
106. Punk, M., Zwerger, W.: Phys. Rev. Lett. **99**, 170404 (2007)
107. Schunck, C., Shin, Y.-I., Schirotzek, A., Zwierlein, M., Ketterle, W.: Science **316**, 867 (2007)
108. Pieri, P., Perali, A., Strinati, G.C.: Nat. Phys. **5**, 736–740 (2009)
109. Schneider, W., Randeria, M.: Phys. Rev. A **81**, 021601 (2010)
110. Barth, M., Zwerger, W.: Ann. Phys. (NY) **326**, 2544–2565 (2011)
111. Braaten, E., Kang, D., Platter, L.: Universal relations for identical bosons from 3-body physics. Preprint arXiv:1101.2854 (2011)
112. Policastro, G., Son, D.T., Starinets, A.O.: Phys. Rev. Lett. **87**, 081601 (2001)
113. Kovtun, P.K., Son, D.T., Starinets, A.O.: Phys. Rev. Lett. **94**, 111601 (2005)
114. Schafer T., Teaney D.: Rep. Prog. Phys. **72**, 126001 (2009)
115. Meyer, H.B.: Phys. Rev. D **76**, 101701 (2007)
116. Balasubramanian, K., McGreevy, J.: Phys. Rev. Lett. **101**, 061601–061604 (2008)
117. Son, D.T.: Phys. Rev. D **78**, 046003–7 (2008)
118. Bruun, G.M., Smith, H.: Phys. Rev. A **75**, 043612 (2007)
119. Cao, C., Elliott, E., Joseph, J., Wu, H., Petricka, J., Schaefer, T., Thomas, J.E.: Science **331**, 58 (2011)
120. Turlapov, A., Kinast, J., Clancy, B., Luo, L., Joseph, J., Thomas, J.: J. Low Temp. Phys. **150**, 567–576 (2008)
121. Rupak, G., Schafer, T.: Phys. Rev. A **76**, 053607–9 (2007)
122. Landau, L., Khalatnikov, I.: Sov. Phys. JETP **19**, 637 (1949)
123. Enss, T., Haussmann, R., Zwerger, W.: Ann. Phys. **326**, 770–796 (2011)
124. Sommer, A., Ku, M., Roati, G., Zwierlein, M.W.: Nature **472**(7342), 201–204 (2011)
125. Chin, C., Bartenstein, M., Altmeyer, A., Riedl, S., Jochim, S., Hecker-Denschlag, J., Grimm, R.: Science **305**, 1128 (2004)
126. Shin, Y., Schunck, C.H., Schirotzek, A., Ketterle, W.: Phys. Rev. Lett. **99**, 090403 (2007)
127. Schunck, C.H., Shin, Y., Schirotzek, A., Ketterle, W.: Nature **454**, 739–743 (2008)
128. Stewart, J.T., Gaebler, J.P., Jin, D.S.: Nature **454**, 744–747 (2008)

129. Campuzano J., Norman M., Randeria M.: Photoemission in the high-tc superconductors. In: Bennemann, K., Ketterson, J. (eds.) The Physics of Superconductors: Vol II: Superconductivity in Nanostructures, High-Tc and Novel Superconductors, Organic Superconductors. Springer, Berlin (2004)
130. Damascelli, A., Hussain, Z., Shen, Z.-X.: Rev. Mod. Phys. **75**, 473 (2003)
131. Chen, Q., Levin, K.: Phys. Rev. Lett. **102**, 190402 (2009)
132. Akkineni, V.K., Ceperley, D.M., Trivedi, N.: Phys. Rev. B **76**, 165116–165116.6 (2007)
133. Magierski, P., Wlazowski, G., Bulgac, A., Drut, J.E.: Phys. Rev. Lett. **103**, 210403 (2009)
134. Norman, M.R., Randeria, M., Ding, H., Campuzano, J.C.: Phys. Rev. B **57**, R11093 (1998)
135. Gaebler, J.P., Stewart, J.T., Drake, T.E., Jin, D.S., Perali, A., Pieri, P., Strinati, G.C.: Nat. Phys. **6**, 569 (2010)
136. Chen, Q., He, Y., Chien, C., Levin, K.: Rep. Prog. Phys. **72**, 122501 (2009)
137. Recati, A., Carusotto, I., Lobo, C., Stringari, S.: Phys. Rev. Lett. **97**, 190403 (2006)
138. Chandrasekhar, B.: Appl. Phys. Lett. **1**, 7 (1962)
139. Clogston, A.: Phys. Rev. Lett. **9**, 266 (1962)
140. Bianchi, A., Movshovich, R., Capan, C., Pagliuso, P., Sarrao, J.L.: Phys. Rev. Lett. **91**, 187004 (2003)
141. Lortz, R., Wang, Y., Demuer, A., Bttger, P.H.M., Bergk, B., Zwicknagl, G., Nakazawa, Y., Wosnitza, J.: Phys. Rev. Lett. **99**, 187002 (2007)
142. Lobo, C., Recati, A., Giorgini, S., Stringari, S.: Phys. Rev. Lett. **97**, 200403–4 (2006)
143. Zwierlein, M.W.A., Schunck, C.H., Ketterle, W.: Science **311**, 492–496 (2006)
144. Zwierlein, M.W., Schunck, C.H., Schirotzek, A., Ketterle, W.: Nature **442**, 54–58 (2006)
145. Shin, Y., Zwierlein, M., Schunck, C., Schirotzek, A., Ketterle, W.: Phys. Rev. Lett. **97**, 030401 (2006)
146. Shin, Y., Schunck, C., Schirotzek, A., Ketterle, W.: Nature **451**, 689 (2007)
147. Gubbels, K., Stoof, H.: Phys. Rev. Lett. **100**, 140407 (2008)
148. Prokof'ev, N., Svistunov, B.: Phys. Rev. B **77**, 020408 (2008)
149. Punk, M., Dumitrescu, P.T., Zwerger, W.: Phys. Rev. A **80**, 053605–10 (2009)
150. Prokof'ev, N.V., Svistunov, B.V.: Phys. Rev. B **77**, 125101 (2008)
151. Schirotzek, A., Wu, C.-H., Sommer, A., Zwierlein, M.W.: Phys. Rev. Lett. **102**, 230402–230404 (2009)
152. Chevy, F.: Phys. Rev. A **74**, 063628 (2006)
153. Combescot, R., Recati, A., Lobo, C., Chevy, F.: Phys. Rev. Lett. **98**, 180402 (2007)
154. Combescot, R., Giraud, S.: Phys. Rev. Lett. **101**, 050404 (2008)
155. Bulgac, A., Forbes, M.M.: Phys. Rev. A **75**, 031605 (2007)
156. Shin, Y.: Phys. Rev. A **77**, 041603–041604 (2008)
157. Nascimbène, S., Navon, N., Jiang, K.J., Tarruell, L., Teichmann, M., McKeever, J., Chevy, F., Salomon, C.: Phys. Rev. Lett. **103**, 170402–170404 (2009)
158. Mora, C., Chevy, F.: Phys. Rev. A **80**, 033607–033610 (2009)
159. Shin, Y., Schirotzek, A., Schunck, C.H., Ketterle, W.: Phys. Rev. Lett. **101**, 070404 (2008)
160. Fulde, P., Ferrell, R.: Phys. Rev. **135**, A550 (1964)
161. Larkin, A., Ovchinnikov, Y.: Zh. Eksp. Teor. Fiz. **47**, 1136 (1964)
162. Bulgac, A., Forbes, M.M.: Phys. Rev. Lett. **101**, 215301–215304 (2008)
163. Fuchs, J.N., Recati, A., Zwerger, W.: Phys. Rev. Lett. **93**, 090408 (2004)
164. Tokatly, I.V.: Phys. Rev. Lett. **93**, 090405 (2004)
165. Liao, Y.-a., Rittner, A.S.C., Paprotta, T., Li, W., Partridge, G.B., Hulet, R.G., Baur, S.K., Mueller, E.J.: Nature **467**, 567 (2010)
166. Huckans, J.H., Williams, J.R., Hazlett, E.L., Stites, R.W., O'Hara, K.M.: Phys. Rev. Lett. **102**, 165302–165304 (2009)
167. Ottenstein, T.B., Lompe, T., Kohnen, M., Wenz, A.N., Jochim, S.: Phys. Rev. Lett. **101**, 203202–203204 (2008)
168. Rapp, A., Zarand, G., Honerkamp, C., Hofstetter, W.: Phys. Rev. Lett. **98**, 160405 (2007)